UNCLASSIFIED

CENTRAL RESEARCH LIBRARY
DOCUMENT COLLECTION

MARTIN MARIETTA ENERGY SYSTEMS LIBRARIES
3 4456 0349842 7

ORNL-1858
Engineering

LOW-POWER CRITICALITY EXPERIMENTS ON THE HOMOGENEOUS REACTOR EXPERIMENT (HRE-1)

S. Visner
P. M. Wood

CENTRAL RESEARCH LIBRARY
DOCUMENT COLLECTION
LIBRARY LOAN COPY
DO NOT TRANSFER TO ANOTHER PERSON
If you wish someone else to see this document, send in name with document and the library will arrange a loan.

OAK RIDGE NATIONAL LABORATORY
OPERATED BY
UNION CARBIDE NUCLEAR COMPANY
A Division of Union Carbide and Carbon Corporation
UCC
POST OFFICE BOX X · OAK RIDGE, TENNESSEE

UNCLASSIFIED

Printed in USA. Price 60 cents. Available from the

Office of Technical Services
U. S. Department of Commerce
Washington 25, D. C.

LEGAL NOTICE

This report was prepared as an account of Government sponsored work. Neither the United States, nor the Commission, nor any person acting on behalf of the Commission:

A. Makes any warranty or representation, express or implied, with respect to the accuracy, completeness, or usefulness of the information contained in this report, or that the use of any information, apparatus, method, or process disclosed in this report may not infringe privately owned rights; or

B. Assumes any liabilities with respect to the use of, or for damages resulting from the use of any information, apparatus, method, or process disclosed in this report.

As used in the above, "person acting on behalf of the Commission" includes any employee or contractor of the Commission to the extent that such employee or contractor prepares, handles or distributes, or provides access to, any information pursuant to his employment or contract with the Commission.

UNCLASSIFIED

ORNL-1858
Engineering
TID-4500 (12th ed.)

Contract No. W-7405-eng-26

Reactor Experimental Engineering Division

LOW-POWER CRITICALITY EXPERIMENTS ON THE HOMOGENEOUS REACTOR EXPERIMENT (HRE-1)

Written by Sidney Visner and Philip M. Wood

Work Performed By:

S. E. Beall	Section Chief
J. J. Hairston	Operations Group Leader
J. W. Hill, Jr.	Operations Group Leader
T. H. Thomas	Operations Group Leader
S. Visner	Experimental Physics Group Leader
D. M. Eissenberg	Reactor Engineer
S. I. Kaplan	Reactor Engineer
V. K. Pare'	Reactor Engineer
P. M. Wood	Reactor Engineer

Work Period Covered; January 1952 through May 1952

DATE ISSUED

MAR 15 1957

OAK RIDGE NATIONAL LABORATORY
Operated by
UNION CARBIDE NUCLEAR COMPANY
A Division of Union Carbide and Carbon Corporation
Post Office Box X
Oak Ridge, Tennessee

MARTIN MARIETTA ENERGY SYSTEMS LIBRARIES

3 4456 0349842 7

UNCLASSIFIED

INTERNAL DISTRIBUTION

1. C. E. Center
2. Biology Library
3. Health Physics Library
4. Metallurgy Library
5-6. Reactor Experimental Engineering Library
7-8. Central Research Library
9-18. Laboratory Records Dept.
19. Laboratory Records, ORNL R.C.
20. G. M. Adamson, Jr.
21. W. L. Albrecht
22. H. F. Bauman
23. S. E. Beall
24. D. S. Billington
25. E. P. Blizard
26. E. G. Bohlmann
27. C. J. Borkowski
28. G. E. Boyd
29. N. C. Bradley
30. R. E. Brooksbank
31. N. A. Brown
32. F. R. Bruce
33. J. R. Buchanan
34. W. D. Burch
35. D. W. Cardwell
36. R. A. Charpie
37. T. E. Cole
38. E. L. Compere
39. D. D. Cowen
40. S. J. Cromer
41. F. L. Culler
42. J. S. Culver
43. N. W. Curtis
44. W. K. Eister
45. J. R. Engel
46. L. B. Emlet (K-25)
47. D. E. Ferguson
48. J. D. Flynn
49. D. F. Frech
50. J. H. Frye, Jr.
51. C. H. Gabbard
52. W. R. Gall
53. T. H. Gladney
54. J. C. Griess
55. J. D. Grimes
56. R. H. Guymon
57. P. H. Harley
58. P. N. Haubenreich
59. J. W. Hill, Jr.
60. A. Hollaender
61. A. S. Householder
62. J. P. Jarvis
63. G. H. Jenks
64. W. H. Jordan
65. R. W. Jurgensen
66. S. I. Kaplan
67. P. R. Kasten
68. C. P. Keim
69. M. T. Kelley
70. A. S. Kitzes
71. J. O. Kolb
72. R. B. Korsmeyer
73. K. A. Kraus
74. J. A. Lane
75. R. E. Leuze
76. S. C. Lind
77. R. B. Lindauer
78. R. S. Livingston
79. M. I. Lundin
80. R. N. Lyon
81. J. P. McBride
82. H. F. McDuffie
83. H. M. McLeod
84. R. A. McNees
85. E. C. Miller
86. K. Z. Morgan
87. E. J. Murphy
88. J. P. Murray (Y-12)
89. M. C. Nelson
90. E. O. Nurmi
91. L. F. Parsly
92. G. W. Rivenbark
93. R. C. Robertson
94. A. M. Rom
95. H. C. Savage
96. H. K. Search
97. C. H. Secoy
98. C. L. Segaser
99. E. D. Shipley
100. A. H. Snell
101. I. Spiewak
102. R. W. Stoughton
103. C. D. Susano
104. J. A. Swartout

105. E. H. Taylor
106. D. G. Thomas
107. D. S. Toomb
108. W. E. Unger
109. R. Van Winkle
110. R. R. Wiethaup
111. A. M. Weinberg
112. K. W. West
113. H. D. Wills
114. C. E. Winters
115. F. C. Zapp
116. ORNL - Y-12 Technical Library, Document Reference Section
117. HRP Director's Office

EXTERNAL DISTRIBUTION

118. R. F. Bacher, California Institute of Technology
119. Division of Research and Development, AEC, ORO
120. F. C. Moesel, Division of Reactor Development, AEC, Washington
121. S. Visner, Combustion Engineering, Inc., Windsor, Connecticut
122-124. Westinghouse PAR Project
125-700. Given distribution as shown in TID-4500 (12th ed.) under Engineering category (200 copies - OTS)

CONTENTS

ABSTRACT 1

I. INTRODUCTION 3

II. DESCRIPTION OF THE EXPERIMENT 7

III. THEORETICAL CALCULATIONS 16

IV. EXPERIMENTAL RESULTS AND DISCUSSION 27

A. Initial Critical Experiment 27

B. Rod Calibration 33

C. Reflector Calibration 37

D. Temperature Coefficient of Reactivity 44

E. Pressure Coefficient of Reactivity 52

F. Inhour Experiments 55

V. SUMMARY AND CONCLUSIONS 59

APPENDICES:

APPENDIX I : Purity of Fuel Solution 62

APPENDIX II : Calculations of HRE Criticality by P. M. Wood ... 64

APPENDIX III : Calculation of Temperature Coefficient of Reactivity 68

REFERENCES 91

LIST OF TABLES

I. Macroscopic Constants for HRE Two-Group Calculations 18

II. Calculated Critical Concentrations of U-235 for the HRE 19

III. Calculated Temperature Coefficient of Reactivity 22

IV. Theoretical Effectiveness of Control and Safety Plates 23

V. Calculated Pressure Coefficient of Reactivity 24

VI. Conditions for Multiplication Measurements in HRE During Initial Criticality Experiment 29

VII. Effectiveness of Controls as Determined from Multiplication Data 32

VIII. Effectiveness of HRE Rods 35

IX. Reflector Calibration at Room Temperature, Fuel Not Circulating 38

X. Reflector Calibration at Room Temperature, Fuel Circulating 39

XI. Reflector Calibration at 220°C by Concentration Change 41

XII. Reflector Calibration by Temperature Change 42

XIII. Critical Fuel Concentrations Below 105°C Without Circulation 46

XIV. Critical Fuel Concentrations with Circulation 48

XV. Effect of Pressure on Reactivity 54

XVI. Static Inhour Data at 28°C 56

XVII. Inhour Data with Circulation of Fuel 57

XVIII. Chemical Impurities in Fuel 63

LIST OF FIGURES

1. Reactor Vessel 71

2. Schematic Flow Diagram 72

3. Arrangement of Safety and Regulating Plates, A 73

4. Arrangement of Safety and Regulating Plates, B 74

5. Thimble for Nuclear Instruments 75

6. Concentration Coefficient of Reactivity 76

7. Multiplication During Initial Critical Experiment 77

8. HRE Control Rod Calibration at Room Temperature 78

9. HRE Shim Rod Calibration 79

10. HRE Reflector Calibration at Room Temperature 80

11. Effectiveness of HRE Reflector at 225°C 81

12. Cooling of Core After Stopping Pump 82

13. Critical Concentrations of HRE Below 105°C 83

14. Critical Concentrations of HRE at All Temperatures 84

15. Temperature Coefficient of Reactivity 85

16. Effect of Reflector Temperature on Reactivity 86

17. Dependence of Reactivity on Pressure 87

18. Inhour Curves for HRE 88

19. Effect of Fuel Concentration on Reactivity 89

20. Calculated Critical Concentration of the Unreflected HRE 90

ABSTRACT

The low power criticality behavior of the HRE has been experimentally investigated and in general, the theoretical predictions were confirmed. The HRE, which is fueled with an aqueous solution of highly enriched UO_2SO_4 in an 18-inch diameter spherical core and reflected by heavy water, was the first prototype of a circulating aqueous homogeneous power reactor and was intended to demonstrate stable operation at high power densities. Criticality was here achieved for the first time in a reactor through which a fluid fuel circulated with the attendant loss of delayed neutrons in the external circuit. It was demonstrated that except for the loss and recovery of reactivity on starting and stopping the circulating pump, the low power behavior of the HRE was qualitatively no different than in a static homogeneous system.

In the main, the criticality data and the various reactivity coefficients agreed well with predictions based on two-group diffusion theory. At room temperature the critical concentration was 24.8 gm U-235/Kg H_2O, and the value of the reflector was 6.5 percent in k_{eff}, which supports a calculated extrapolation distance of 4 cm on the unreflected core radius. The temperature coefficient of reactivity at room temperature was minus 0.37×10^{-3} k_{eff} per degree centigrade while at 220°C the value was minus 1.15×10^{-3} k_{eff} per degree centigrade. The temperature coefficient for the reflector was only minus 2.5×10^{-5} k_{eff} per degree centigrade. The pressure coefficient of reactivity for the core was 0.18 percent k_{eff} per thousand psi.

The effectiveness of the control, shim, and safety rods together in Δk_{eff} was 1.3 percent at room temperature and 1.6 percent at 200°C. The decrease in

the effective delayed neutron fraction on circulation was 0.20 percent k_{eff} as indicated by direct measurement of the change in reactivity and as also indicated by the inhour relationship.

I. INTRODUCTION

The Homogeneous Reactor Experiment was the first reactor prototype incorporating a circulating homogeneous aqueous fuel operating at high specific power and temperature, with the reactor coupled to a steam turbine generator. The reactor was built for the purpose of demonstrating the feasibility of this concept; primarily to show that the reactor was self-regulating and inherently stable.

The reactor consisted essentially of an 18-inch diameter spherical core inside a 39-inch diameter reflector vessel, a circulating pump, and a heat exchanger where steam was produced for the operation of the turbine generator. The design conditions were 250°C temperature, 1000 psig pressure, and 1000 Kw reactor power. The material of construction was type 347 stainless steel. A low pressure system contained dump tanks for the storage of fuel solution, an evaporator and condensate tanks for changing concentration, and recombiners for the decomposition gases released in the core. The fuel was a light water solution of UO_2SO_4 with a U-235 enrichment of 93 percent and the reflector was heavy water. Extensive calculations had been made for the purpose of predicting the nuclear behavior of the reactor, and these served as a guide in the building and experimental testing of the reactor.

Experimental Program

An experimental program was formulated for the purpose of investigating the important problems associated with the HRE:

1. Nuclear Control and Stability. Of special interest were the effects of coupling the reactor to an electrical power production unit, effects of circulating the fuel with the resulting loss of delayed neutrons, and the effects of

gas production from the dissociation of water. Owing to the predicted large negative temperature coefficient, it was expected that the reactor would be self-stabilizing, capable of absorbing large reactivity changes, and also capable of being controlled by power demand alone. The dynamic properties of the reactor could only be checked under conditions of high power operation where significant quantities of heat and gas are generated, and this was the ultimate objective of the experimental program. An analysis of the operation of the reactor at design power will be given in later reports.

2. Low Power Static Measurements. To facilitate the operation of the reactor at high power and also to interpret the high power performance, it was decided to obtain such fundamental reactor physics data as the reactivity control of the rods and reflector level, temperature and pressure coefficients of reactivity, and effective delayed neutron fraction. For example, the temperature coefficient of reactivity and effectiveness of the reflector determined the temperature at which the reactor would again become critical, as it cooled after a shutdown in which the reflector was dumped. Another objective of these experiments was to check the reliability of the two-group diffusion approximation and constants which were used in the design calculations. The bulk of the calculations for the HRE appear in the feasibility and progress reports. However, some are more recent and are presented in somewhat more detail in this report along with the results of the earlier calculations.

These measurements could best be obtained with the reactor critical at low power (less than one watt) to avoid the complicating factors of gas bubbles, temperature distribution in the core, and anomolous fuel concentration effects.

Additional advantages of low power operation were anticipated in the relative ease of making repairs and revisions to the system in the absence of induced activity and also the higher accuracy in the analytical determinations of fuel concentration which is possible when the fuel has not been activated. The present report is primarily concerned with the experiments on reactor statics which were performed at low power.

3. Engineering Performance. The performance of pumps, heat exchangers, valves, and instruments in the chemical and radiation environment of the reactor are important to the designers of large plants. This information will be issued in a separate report.

4. Chemical and Corrosion Data. At the same time that the above information was obtained, studies were made of the chemical stability of the fuel solution, the corrosion of the 347 stainless steel, and the internal recombination of the radiolytic gases by copper in solution. This information will also be reported separately.

Basic Philosophy for Low Power Experiments

The basic philosophy in programming the reactor physics experiments called for performing the simplest experiments first in a straight-forward manner. This was dictated by considerations of safety and of ease in interpreting the data. In line with this philosophy, the initial critical experiment was performed at room temperature on a static system consisting essentially of the reactor vessel and the circulating pump for mixing purposes only. Next, criticality was achieved with the fuel solution circulating at 120 gpm, corresponding to a residence time of 6 sec inside the core and 2 sec outside. In due time,

the reactor system was connected together as intended for high power operation and made critical with the additional complexity of recirculation of the fuel between the high pressure system dump tanks, injection of oxygen into the fuel stream, and with the operation of the concentration control system.

In following sections are presented a description of the essential features of the reactor, data obtained on the effectiveness of the rods and reflector, critical concentration as a function of temperature, pressure coefficient of reactivity, and inhour data. A comparison is made between the experimental data and the theoretical predictions. It is intended to report in a later document the experiments at high power operation.

II. DESCRIPTION OF THE EXPERIMENT

A detailed description of the engineering design, instrumentation, and construction of the HRE as a power producing machine has already been given in previous reports.[1,2,3,4] A brief description will here be given only of the features which are pertinent to the discussion of the low-power critical experiments.

The Reactor System

The chain reaction occurred in a light water solution of enriched uranyl sulfate contained in a 50 liter spherical core vessel, 18 inches I.D. and 3/16 inch thick, Figure 1. This was surrounded by a heavy mild-steel pressure vessel, 39 inch I.D. and 3 inches thick, accommodating a reflector region of D_2O, 10 inches thick. The fuel solution was normally circulated at 120 gpm through the core and then through the tubes of a heat exchanger by means of a centrifugal pump constructed with a canned rotor, Figure 2. All equipment in contact with the solution was made of type 347 stainless steel. The solution entered the core near the equator with a tangential flow velocity creating a rotational flow pattern for the purpose of centrifuging towards a central vortex the gas bubbles which were formed at high power. Gas and solution were removed from the top of the vortex to the low-pressure system, the rate being controlled by the liquid level in the pressurizer stem directly above the core. For low-power experiments, the fuel solution was heated to any temperature up to 250°C by admitting steam to the shell side of the heat exchanger. This of course was just the reverse of normal operation at high power when water was injected and steam removed from the heat exchanger. For the earliest experiments--up to the time

that the low-pressure and high-pressure systems were tied together--the desired reactor pressure, usually 100 psig, was maintained by means of helium. Later, the reactor was pressurized with steam by heating the pressurizer stem with steam at the appropriate temperature.

The low-pressure fuel system consisted of storage tanks; an evaporator, condenser, and condensate storage tanks for controlling concentration; recombiners for the radiolytic gases produced at high power; cold traps for drying the waste gas; charcoal beds for absorbing and delaying the fission product gases, and finally a 100 ft stack for venting to the atmosphere. All water not retained in the condensate storage tanks was returned to the fuel storage tanks from which fuel solution was continually pumped into the high pressure system at one gpm. Normally, oxygen was injected into this stream at 20 standard cc/sec for the purpose of keeping the uranyl ion in its oxidized (soluble) state.

Volume of Equipment

The capacities of the major items of equipment in liters were as follows:

Core	50.0
Pressurizer and connecting stem	5.1
Main heat exchanger	5.5
Circulating Pump	1.3
Pipes in circulating system	8.8
Miscellaneous lines	1.3
Total in high pressure system	72.0 liters

Fuel dump tanks	285 liters
Condensate storage tanks	150 liters
Reflector region around core	480 liters
Reflector dump tanks	614 liters

Fuel Solution

The isotopic content of U-235 in the uranium was nominally 93 percent by weight. In the course of the initial critical experiment at room temperature, the U-235 content decreased from 93.13 percent to 92.54 percent, which was attributed primarily to the pick-up of approximately 10 gm of normal uranium which had been deposited in the film on the piping during the period of pre-operational testing with UO_2SO_4 solution of normal isotopic content. This hypothesis is supported by measurements on the uranium content of films developed during out-of-pile corrosion tests.* No further decrease in U-235 assay was ever observed, although the system was later operated at temperatures up to 250°C.

The UO_2SO_4 solution was of relatively very high purity. The mole ratio of UO_2 to SO_4 was within one percent of unity. The total macroscopic absorption cross-section for thermal neutrons of extraneous ions in the fuel, as determined from spectrographic analysis, was only five percent of that for the sulfate ions and was therefore negligible. This data is given in some detail in Appendix I. In the course of the low-power experimental program, the nickel which accumulated in solution from the corrosion of the stainless steel contributed no more than 6 percent of the sulfate cross-section.

---

* Personal communication from J. C. Griess, Corrosion Section, Homogeneous Reactor Project

Since the concentration of U-235 in solution was the fundamental measure of reactivity, considerable effort was made to obtain high accuracy in the sampling and analysis. In the course of the fundamental reactivity calibrations for the reactor, samples of the fuel solution from the high-pressure circulating system were removed in 25 ml sample bombs after allowing for adequate flushing of the bomb and sample connections. This arrangement, temporary in nature, was installed for the purpose of removing large samples and also for adding concentrated UO_2SO_4 solution to the high pressure system to increase the U-235 inventory. Aliquots were analyzed in triplicate by gravimetric determinations of U_3O_8. Often duplicate sample bombs were withdrawn, and also aliquots from the same sample were checked at different analytical laboratories. From an analysis of the variability of such data and also the variability of results on a standard solution of UO_2SO_4, the accuracy in the sampling and analysis combined is estimated as 0.4 percent probable error for any one sample.

In preparing the reactor for high-power operation, the temporary sampling equipment was removed on October 13, 1952 and a sampler which provided for remote manipulation was installed. Although the isolation chamber in this sampler had a capacity of 20 ml, only one-half ml could be withdrawn with the sampling mechanism. The uranium content of the small sample was determined by potentiometric titration. In an effort to improve the accuracy for the critical experiments at core temperatures from 217°C to 230°C, the entire contents of the isolation chamber were removed with a pipette by hand operation. The error here however was still found to be several times greater than obtained earlier with the sample bombs.

It was also possible to estimate the fuel concentration from the inventory of U-235 and water and hold-up of condensate. However, when the leakage of solution and steam from the reactor to the outer dump tanks through worn valve seats became troublesome, it was no longer feasible to infer the concentration by this method.

Heavy Water Reflector

The D_2O in the reflector system was monitored for changes in light water content by density measurements on samples. No significant trend was detected in the nine analyses made which gave a mean value of 96.6% D_2O with a standard deviation of 1.1%. It is believed that density measurements would give significant indications of trends but not necessarily of the absolute value of the purity. A determination by mass spectrometer at the conclusion of the reactor program gave 99.1 weight percent D_2O. The effect at 20°C of a one percent H_2O impurity was calculated to be only 0.10 gm U-235/Kg H_2O or 0.15 percent k_{eff}.

Reactivity Controls

The reactivity in the HRE was controlled in any of several ways: temperature and concentration of the fuel, level of the reflector, and position of poison rods.

Fuel Concentration. As described earlier, the fuel solution could be concentrated by removing condensate at rates up to 0.5 Kg/min and storing the condensate in two tanks which are suspended from weighing cells. The equivalent reactivity increase at 200°C is 0.005 percent per sec. Dilution was achieved by draining the condensate back into the dump tanks.

Reflector Level. The reflector level was raised by pumping D_2O from the

dump tanks with a diaphragm pump at a rate up to 2 gpm, corresponding to 0.36 inches per minute in level or 0.003 percent k_{eff} per sec. The D_2O could be drained slowly through a let-down valve or dumped completely within 8 seconds by opening a two-inch dump valve. A liquid-level recorder and controller were provided for routine operation. During the low power experiments, when greater accuracy was desired, the reflector level was also measured directly by means of a manometer.

Control Plates. Three poison plates, designated as control, shim, and safety rods were located vertically in the reflector region, adjacent to the core. The rods were constructed of boral sheet--weight composition: 80.1% 2S aluminum and 19.9% B_4C--0.0625 inches thick, enclosed in a jacket of type 347 stainless steel which was 0.038" thick. The surface density of boron was 0.063 gm/cm^2 yielding a capture cross-section for thermal neutrons at 20^oC of 2.5 cm^2/cm^2 of surface. The shim and safety rods were identical, Figures 3 and 4, consisting of four plates, each curved about a 120 degree sector, with successive plates recessed in such a manner as to follow the contour of the core. Each rod, when fully inserted, covered approximately one-sixth of the core, with the bottom of the rod 3 inches below the equator. In the withdrawn position, the bottom of the rod was at the same elevation as the top of the core. The control plate was constructed in one piece forming a 105 degree arc of a right circular cylinder, 9.5 inch radius and 9 inches high. The bottom of the control rod, when fully inserted, was 1-3/8" below the core equator, and when withdrawn was 1-5/8" above the top of the core.

The rods could be raised and lowered at a rate of four inches per minute

or 0.004 percent k_{eff} per sec by means of a vertical drive screw which was driven by a gear motor. The number of revolutions of the drive screw--a revolution produces 0.05 inches vertical travel--was registered at the operating console. The shim and safety plates were coupled to the drive mechanism through a magnetic clutch which was energized through the nuclear safety circuits. In the process of coupling, a spring was compressed with a force of 100 pounds to provide sufficient acceleration to insert the plates within 0.2 seconds after release by the magnet.

Fuel Temperature. As mentioned earlier, the temperature of the fuel solution in the core could be controlled when circulating by introducing either steam or cold water to the shell side of the heat exchanger. The temperature was changed no faster than 40°C per hour which was dictated by considerations of thermal stresses in the equipment. Since there was no access to the core itself, the temperature was measured by means of thermocouples attached to the main circulation pipes, both at the core inlet and outlet. These measurements were valid of course only when the fuel was circulating.

Nuclear Instrumentation

The thermal neutron flux was monitored by means of chambers which were located in six thimbles penetrating the shield and reflector region;[3] figure 5 shows the details of a typical thimble. The nuclear instruments and circuits are very similar to those used in the MTR.[5]

Fission Chambers. Two fission chambers with associated type A-1A preamplifiers and A-1 amplifiers were connected both to scalers and to strip recorders which had a logarithmic scale of four decades. These chambers were

most useful in approaching criticality since they were sufficiently sensitive at neutron source power of the order of 10^{-5} watts. The range of the instruments was increased as necessary by as much as a factor of 10^4 by withdrawing the chamber within the thimble.

Safety Chambers. Two ionization chambers containing boron were connected to linear amplifiers and recorders and were used to monitor the power in the range from 10^{-3} to 10^6 watts. This was achieved by the combination of moving the chamber in the thimble and selecting a grid input resistor from the values 4×10^5, 10^6, 10^7, and 10^8 ohms.

Compensated Chamber. One boron chamber which was compensated for gamma radiation was used in conjunction with a logarithmic amplifier and a reactor period amplifier. The period was indicated on a console meter while the neutron level was recorded on a logarithmic chart of 6.5 decades. The range of this instrument was adjusted only by moving the chamber, the lowest power being of the order of one watt and the highest, of the order of 100 megawatts. During the high power operation of the HRE, frequent changes in compensation were needed due to the build-up of gamma sources in the reactor components.

Nuclear Safety Controls

Although calculations had indicated that the HRE was self-stabilizing and inherently safe, caution dictated that safety controls be installed. When it was later demonstrated that they were not needed, these controls were inactivated.

The outputs from the amplifiers for both safety chambers and from the period amplifier for the compensated chamber were fed into individual Sigma amplifiers. The output from these amplifiers independently controlled the current to the magnets holding the shim and safety rods and also controlled the dumping of the D_2O reflector. At the first scram level, the rods were dropped

and the timer started which in 30 seconds initiated the dumping of the reflector. The operator could at his discretion prevent the dump from occurring by holding a switch until the situation was rectified. At a second scram level corresponding to higher flux level and/or shorter period, the reflector was dumped without delay.

III. THEORETICAL CALCULATIONS

The more important reactor constants for the HRE had been calculated from theory for the purpose of designing the reactor and predicting its behavior. These constants included the critical fuel concentration, the temperature coefficient of reactivity, the effectiveness of the D_2O reflector and rods, and the effective delayed neutron fraction with the fuel circulating.

A. Critical Concentration of the Reflected Reactor

The critical concentration of the reflected reactor was calculated from two-group diffusion theory for the two-region spherical geometry consisting of the core and reflector. The earliest estimate was made by Stein[1] who took into account the stainless steel core tank, 3/16" thick, by including its absorption of thermal neutrons into the boundary condition for the slow neutron current at the core-reflector interface. The critical concentrations for core temperatures from 20° to 250° at a constant reflector temperature of $100^{\circ}C$ were calculated by this method. The temperature affects the reactor constants in two ways: through the density of the solution and through the dependence on neutron velocity, v, of the microscopic cross sections. Stein took the thermal absorption and fission cross sections to vary as v^{-1} and the hydrogen scattering cross section to vary as $v^{-0.6}$.

Criticality calculations were also made by Welton[6] and Wood[7] using a short-cut approximation to the two-group method, based on the work of R. P. Feynman and T. A. Welton.[8] The steel core shell was treated as an additional region which attenuated the thermal neutrons but did not affect the fast neutrons.

The macroscopic constants used by Stein and Welton are given in Table I. It is significant that for both the fast and slow neutron groups, the diffusion

constants for the core and reflector enter the calculations only as their ratio. Stein's diffusion constants had been successfully used previously by Spinrad and Greuling[9] in criticality calculations for U-235-D_2O systems. The nuclear data for the uranium isotopes were essentially the same as compiled by the AEC cross-section group.[10]

The ratio of fast diffusion constants used by Welton and Wood were also obtained from reference (9). The values at room temperature for the thermal diffusion length, however, along with the thermal absorption cross-section for water, $\sigma_a(H_2O)$, used by Welton were obtained from reported measurements on the diffusion in a tank of water of neutrons from a thermal beam.[11] In this experiment, the neutrons are not mono-energetic but possess a velocity distribution which is probably not too different from Maxwellian. It is probably for this reason that the value obtained for $\sigma_a(H_2O)$, 0.69 barns, is considerable higher than the more accepted value of 0.64 barns for the neutron speed of 2200 meters per sec. Wood used the same value for the thermal diffusion length as Welton but took the cross-section for H_2O at 2200 meters per sec, as was done for the uranium, on the basis that the cross-sections enter most strongly into the criticality equation as their ratio. The calculated critical concentrations are presented in Table II.

TABLE I

MACROSCOPIC CONSTANTS FOR HRE TWO-GROUP CALCULATIONS

Moderator	Temp. °C	Slow Diffusion Constant (cm)		Square of Slow Diffusion Length (cm^2)		Fast Diffusion Constant (cm)	Fermi Age (cm^2)	
		Stein	Welton	Stein	Welton	Stein and Welton	Stein	Welton
	20	0.142	0.161	6.62	7.07	1.14	33.0	33.0
H_2O	175	.180	.210	11.50	12.77	1.28	41.1	41.3
	250	.211	.250	16.39	18.44	1.43	51.2	52.2
	20	.80	.91	1.00×10^4	1.51×10^4	1.13	120	120
D_2O	100	.86	-	1.26×10^4	-	1.18	130	-
	175	-	1.10	-	2.53×10^4	1.27	-	153

UNCLASSIFIED

TABLE II

CALCULATED CRITICAL CONCENTRATIONS OF U-235 FOR THE HRE

Temp °C	Critical Concentration with D_2O Reflector, gm/Kg H_2O			Critical Concentration No reflector, gm/Kg H_2O			Reflector Effectiveness* k/k, per cent		
	Stein	Welton	Wood	Stein	Welton	Wood	Stein	Welton	Wood
20	26.0[a]	-	24.8[c]	48	52.9	31.2	15.7	-	7.5
230	-	40.1[b]	-	-	300	-	-	24.5	-
250	38.4[a]	-	41.3[b]	192	-	59.7	20.7	-	11.2

Note: The effect of the 3-inch thick pressure vessel for the reflector, about one percent in k_{eff}, is not included in the calculations.

* Reduction in k_{eff} of the bare reactor using the critical concentration of the reflected reactor.

a. Reflector temperature, 100°C

b. Reflector temperature, 175°C

c. Reflector temperature, 20°C

The calculated critical concentrations are naturally dependent on the choice of constants. In fact, an increase in the ratio of the fast diffusion constants, reflector to core, from 1.00 to 1.25 increases the critical concentration by approximately 10 per cent.

B. Effectiveness of Reflector

The effectiveness of the reflector is the difference in critical fuel concentration for the reflected and bare reactor. The critical concentration of the unreflected core was obtained by the usual two-group criticality equation. For the purposes of this report, the reactivity effectiveness of the reflector is numerically equal to the reduction in k_{eff} of the bare reactor when the concentration is reduced to the critical concentration of the reflected reactor.

For a reactor of the dimensions of the HRE, the results are quite sensitive to the choice of the extrapolation distance. From transport theory, the extrapolation distance is 0.71 times the transport mean free path, λ_{tr}, which in turn is three times the diffusion constant. Apparently, in the calculations by Stein and Welton, a negligible extrapolation distance was used. However, in subsequent calculations by Wood, presented in Appendix I, an extrapolation distance of 4 cm was selected at 20°C based on a calculated value of 1.9 cm for the fast diffusion constant in H_2O.*

---

* The fast diffusion constant was here obtained as the product of the empirical age (square of the characteristic slowing down length), and the macroscopic cross-section for the removal of neutrons from the fast group by thermalization; this cross-section being the ratio of macroscopic fast scattering cross-section to the average number of collisions required to thermalize a fission neutron. In calculating the average fast scattering cross-section, the assumption was made that the assymptotic distribution of neutron flux with energy holds. Approximately the same value of D_f was obtained by assuming that the energy distribution of the flux is inversely proportional to the energy.

The effect on reactivity from the return of fast neutrons to the bare core by the 3-inch thick steel pressure vessel has been calculated to be approximately one per cent in k_{eff}. The result is to decrease by one per cent k_{eff} the reactivity effect calculated for draining the D_2O reflector.

The relationship between reflector effectiveness and the D_2O level in the reflector vessel can be obtained from elementary considerations. To a first approximation, the effectiveness of the reflector when the core is immersed should increase linearly with the level of the D_2O in the reflector level since the surface of the core that is immersed in D_2O is proportional to the reflector height. This follows from the geometrical property of spheres that the surface area of the sphere subtended by an intersecting plane is linearly dependent on the distance from the plane to the center of the sphere.

C. Temperature Coefficient of Reactivity

The temperature coefficient of reactivity is the change in k_{eff} for each degree centigrade. Stein fitted a polynomial of the third degree in temperature to the critical infinite multiplication constants he calculated in the temperature interval 20° to $250^{\circ}C$; and by differentiation, he obtained the temperature coefficient. Welton and Wood calculated the coefficient from the difference in k_{eff} at two temperatures for the same concentration. The temperature coefficient can also be obtained more directly by differentiating the criticality equation for an equivalent bare sphere (Appendix III); the buckling of the equivalent bare sphere is that required for criticality with the same critical fuel concentration as the reflected reactor. The variation of U-235 absorption cross-section[12] with neutron energy, E, was taken as $E^{-1.2}$. It is apparent from Table III, where the calculated temperature coefficients are listed, that at room temperature the

contribution to the coefficient from the variation in cross-section is comparable to that from the density change. At 250°C, however, the cross-section effect is less than 10 percent of the density effect.

TABLE III

CALCULATED TEMPERATURE COEFFICIENT OF REACTIVITY

$\partial k_{eff}/^{o}C \times 10^{3}$

Temp. °C	Stein	Welton	Wood	Nuclear and Density Effect	Nuclear Only
20	0.12	-	0.44	0.32	0.21
100	.43	-	.63	.64	.19
175	.61	-	.86	.93	.16
230	-	0.94	-	-	-
250	.71	-	1.48	1.56	.14

D. Safety Plates

The effectiveness of the control, shim, and safety plates were calculated by Stein by means of a perturbation method[1] where the two-group neutron fluxes and adjoint fluxes calculated for the reactor without rods were used as weighting functions. It is to be expected that by this method, the value of the plates would be overestimated since the presence of boron in the concentration and quantity existing in the plates is bound to depress the flux in the region of the plates. The effectiveness of the plates was calculated by Wood[4] from the change in reactivity to be expected when an absorbing curtain, which is black to thermal neutrons and transparent to fast neutrons, is interposed between the

core and reflector. The value for the rods was then obtained from the fractional solid angle they subtend at the core. Results obtained by both methods are presented in Table IV where it is apparent that the perturbation method gives a value 2.5 times greater than the "absorbing curtain" method. The total value of all rods by the latter method is 3.9 percent at 250°C.

TABLE IV

THEORETICAL EFFECTIVENESS OF CONTROL AND SAFETY PLATES

Temp. °C	Safety Plate, k_{eff} Perturbation Method	Safety Plate, k_{eff} "Absorbing Curtain" Method	Control Plate, k_{eff} "Absorbing Curtain" Method
20		1.05%	0.77
250	4%	1.44%	1.06

E. Pressure Coefficient

The pressure in the core affects the reactivity in two ways: through the density of the solution and through the stretching of the core vessel. Both reactivity effects have been calculated directly from the criticality equation for the equivalent bare sphere and are presented in Table V. The effect due to stretching the core tank is very small and if the radius of the equivalent bare sphere were arbitrarily taken as equal to the geometrical radius of the core to obtain an upper bound, the values shown would be increased by no more than 50 percent.

TABLE V

CALCULATED PRESSURE COEFFICIENT OF REACTIVITY, $\frac{\partial K_{EFF}}{\partial P}$

Temp. °C	Density Effect; Core and Reflector Pressure Balanced	Tank Stretching Effect; Reflector Pressure Constant
30	0.16%/1000 psi	0.21%/1000 psi
250	0.57%/1000 psi	0.63%/1000 psi

F. Fuel Concentration as a Measure of Reactivity

The effective multiplication of the reactor is determined uniquely by the fuel concentration for any specified temperature, reflector, and control rod position. A change in reactivity produced in any fashion can very conveniently be measured by the corresponding change in fuel concentration which is required to return the reactor to delayed critical. In considerations of reactor kinetics, however, the reactivity or effective multiplication constant enter directly.

However, at times it is desirable to use reactivity or effective multiplication constant directly since they enter into the kinetics of the reactor. Furthermore, comparisons with other reactors can be made more conveniently with these units. Reactivity is a quantity however that cannot be directly measured but may be inferred from the manner in which the reactor departs from equilibrium after some change is made in the reactor. Unfortunately, success here depends on accurate knowledge of the effective delayed neutron fractions--including the photo-neutrons from the D_2O--and the prompt neutron generation time. Another approach is to determine empirically the equivalence between fuel concentration and reactivity by means of a boron bubble experiment[13] where the only

uncertainty is the value for the absorption cross-section for boron. The necessary facilities for such an experiment were not available in the HRE, which was designed primarily as a reactor for producing power at high temperature and pressure.

The alternative, which proved successful, was a calculated conversion between fuel concentration and k_{eff} by the Feynman-Welton approximation to diffusion theory. According to their formulation, the concentration enters primarily in the thermal utilization, f, and in the leakage term for slow neutrons $(1 + L^2B^2)$, through the square of the slow neutron diffusion length, L^2. Essentially, the criticality equation for the reflected reactor can be reduced to that for a single region with an appropriate value for the buckling, B^2, thus

$$k_{eff} = \frac{\eta f p}{1 + L^2 B^2} A,$$

where at constant temperature, the resonance escape probability, p, and the factor A are essentially constant over the range of concentration of interest in the HRE.

After introducing the explicit expressions for L^2 and f in terms of the concentration, C, one obtains

$$C = \left(\frac{\eta A}{k_{eff}} - 1\right) = \text{Constant}$$

The conversion between effective multiplication and concentration then becomes, for k_{eff} equal to unity,

$$\frac{\partial k_{eff}}{\partial C} = \frac{\eta A - 1}{C_{cr}\, \eta A}$$

where C_{cr} is the critical concentration and can be obtained by direct measurement. For any temperature, the value of A is obtained from the measurement of critical concentration and from the value of B^2 calculated from theory. The dependence of A on B^2 is through a term $(1 + L_o^2 B^2)$ and since $L_o^2 B^2$ for the HRE is of the order of 0.1, the effect of approximations in the theory is correspondingly reduced. The applicability of the theory in this treatment is borne out by the success in predicting the critical concentrations of the HRE. The values of $\partial k_{eff}/\partial C$ derived by this method are plotted in Figure 6 as a function of the temperature.

IV. EXPERIMENTAL RESULTS AND DISCUSSION

A. Initial Critical Experiment

Summary. As is customary in attaining criticality for the first time with a new system, a cautious empirical approach was used in bringing the HRE to a "zero power" critical condition on April 15, 1953. The fuel was added in steps while finer control of reactivity between steps was obtained with the reactor controls: shim and control rods, and reflector level. A plot was maintained of the neutron multiplication, or rather reciprocal counting rate, as a function of fuel concentration in order to predict safe values for successive fuel additions, and also to obtain an early estimate of the reactivity controls. The fuel concentration was obtained from the inventory of U-235 and water in the system and was checked by chemical analyses of samples removed after each fuel addition. After 30 fuel additions over a period of two days, criticality was achieved at a temperature of 30°C with a fuel concentration of 24.9 grams of U-235 per Kg of water, which is within one percent of the theoretical prediction.

Description of Experiment. The initial criticality experiment was performed in the high pressure circulating system which consisted essentially of the 18-inch diameter spherical core, the heat exchanger, the circulating pump of 120 gpm capacity, and temporary lines for filling and sampling. All lines normally connecting the high pressure circulating system to the low pressure system were blanked off, except for the dump line which was retained as a last resort safety device.

The pump was used only as a means of mixing the solution in the system after a fuel addition. The sample bombs were connected across the heat exchanger to

obtain adequate circulation through the bombs.

Approximately 70 Kg of water were first added to the high pressure system through the temporary filling line, bringing the level in the pressurizer approximately six inches above the fuel outlet connection. In this manner, it was planned to minimize any mixing effects introduced by the region above this point which has a volume of approximately 6 liters. The flanges on the two blanked-off lines were temporarily loosened in order to vent the lines while filling. Earlier tests with normal uranyl sulfate solution had indicated that the mixing the system would be satisfactory, and this was borne out during the critical experiment where the neutron multiplication was a rapid and sensitive indication of changes in concentration.

For the purpose of adding fuel, the sample bombs which were of two sizes, 75 ml and 300 ml, were filled with a predetermined quantity of stock UO_2SO_4 solution. After a bomb was connected to the sampling lines, the circulating pump was turned on for 10 minutes. The sample bomb was then removed from the sampler point after isolation, containing a representative sample of the fuel solution. In this manner, the procedure of adding fuel and withdrawing a sample did not change the volume of fuel solution in the system.

The reactor was prepared for each loading by lowering the reflector to the top of the core, inserting the control and shim plates, and cocking the safety plate. In this manner, a reduction was made in reactivity of 1.3 per cent which is equivalent to 0.9 gm U-235 per Kg of water when critical. This corresponded to a change in mass of U-235 in the system of 65 gms as compared to limit of 45 gms which was imposed on the size of additions after approximately two-thirds of the required uranium had been introduced into the reactor. The earlier additions

were limited to about 100 gm batches with the neutron count rates determined between every two or three batches. Data on neutron multiplication was obtained with the two fission chambers which were connected both to scaling units and recorders and also with the graphite ionization chamber connected to a recorder, for the static conditions listed in Table VI.

TABLE VI

CONDITIONS FOR MULTIPLICATION MEASUREMENTS IN HRE DURING INITIAL CRITICALITY EXPERIMENT

Condition	Reflector Level	Rods		
		Control	Shim	Safety
1	Top of Core	In	In	Out
2	Full	In	In	Out
3	Full	In	Out	Out
4	Full	Out	Out	Out
5	Full	In	In	In

A plot of reciprocal counting rate as a function of concentration was kept for each of these conditions in order to predict when criticality would be reached and also to obtain an early estimate of the effectiveness of the controls. On occasions, the multiplication was followed as the reflector level was varied between completely empty and full.

Effect of Circulation. It was apparent fairly early in the experiment that the decrease in neutron multiplication from the circulation of the fuel was greater than expected on the basis of the reduction in the effective delayed neutrons. For example, when a fuel concentration in the reactor of 21 gms per Kg of water was reached, the decrease was approximately 7 percent in the

multiplication factor of about 15, corresponding to a reactivity change of 0.5 percent as compared to 0.2 percent predicted. This anomoly was caused by air being sucked into the solution from the free surface close to the outlet line in the pressurizer stem, the air then decreasing the average fuel density in the core. After an additional 1.23 Kg of water was added, raising the level in the pressurizer stem by 11 inches, the change in reactivity resulting from circulation was reduced by one-half, bringing it in line with predictions.

Multiplication Data: The apparent multiplication, which is the ratio of the initial counting rate with pure water in the reactor to the counting rate observed with fuel solution, is shown in Figure 7 for the reactor with the reflector full and all rods withdrawn. The solid curve is the multiplication calculated from two-group diffusion theory. The agreement between the curves is remarkably good in view of the fact that the apparent multiplication measured with the detectors is not the true multiplication of the reactor. The difference between true and apparent multiplication arises from two factors: the relative distribution of neutron flux through the reactor which depends on the degree of excitation of higher modes varies with the reactivity or fuel concentration; also, the detectors respond to some neutrons originating from the Po-Be source as well as from the reactor, and the ratio of the two contributions also depends on the reactivity.

Criticality was reached at the concentration of 24.9 gms U-235 per Kg H_2O, with the reactor full, shim and safety plates completely out and the control rod withdrawn 3.6 inches. From later work on calibrations of the control plate, it was determined that the equivalent critical concentration with all rods out is 24.8 which is within one percent of the value of 25.1 calculated from two-group

diffusion theory. For each condition listed in Table VI, the curve of reciprocal counting rate as a function of fuel concentration obtained with the three detectors was slightly convex toward the origin. From an experimental point of view, this shape for the curves is to be preferred since the extrapolations for the critical concentration give conservative predictions.

As mentioned earlier, estimates were made in the course of the initial critical experiment of the value of the reactivity controls from the multiplication data obtained with the south fission chamber which had the best geometry. The estimates from differences in multiplication are presented in Table VII along with estimates made at the conclusion of the experiment from the critical concentrations to which the reciprocal count rate curves extrapolated. Also shown for comparison are the more accurate values of reactivity controls obtained later by direct calibration in terms of reactor period and critical fuel concentration.

TABLE VII

EFFECTIVENESS OF CONTROLS AS DETERMINED FROM MULTIPLICATION DATA

Fuel Conc. g U-235/Kg H_2O	Control Rod Δk_{eff}, %	Shim Rod Δk_{eff}, %	Control Shim and Safety Rods Δk_{eff}, %	Reflector Level From Top of Core to Full Δk_{eff}, %
20.0	0.3	1.6	3.5	1.0
21.3	.3	1.3	2.8	3.0
22.8	.2	.9	1.8	1.9
23.9	.2	.6	1.3	1.1
24.8	.2	.3	.9	.7
Extrapolation of Multiplication Curves	.3	.5	1.3	.7
Calibration from Criticality Data	.32	.48	1.28	.6

In general, the magnitude of the estimates from the multiplication data decreased with successive fuel additions, approaching the values determined more accurately later by criticality measurements. The large uncertainty in the estimates at the lower multiplications undoubtedly reflects the difference between the apparent and true multiplication and also geometry effects associated with moving the rods and reflector, both effects decreasing as criticality is approached. However, the estimates obtained from extrapolations of the multiplication curves agreed very well with the values from direct calibration.

It was not possible to determine the effectiveness of the entire reflector from neutron multiplication measurements since large changes in reflector level radically altered the geometry of the system, changing the relative efficiency

of the detectors to neutrons eminating from the source and to neutrons multiplied in the reactor. For example, as the reflector level was raised to a point above the bottom of the core where the instrument thimble in which were located the neutron detectors became immersed in D_2O, a sharp increase in count rate was observed. For fuel concentration as dilute as 16 gms of U-235 per Kg of H_2O, this was followed by a decrease in count rate as the reflector level was raised further and finally by an increase in count rate as the neutron source, which was located near the top of the core, became immersed.

B. Rod Calibrations

The first step in the experimental program after the initial critical experiment was the calibration of the control and safety mechanisms. The control and shim rods were calibrated at room temperature by two methods: by measuring the pile period associated with a change in rod position; and by measuring the change in fuel concentration required to maintain the reactor critical. The value of the safety rod which was kept in a cocked position at all times was taken to be equal to that of the shim rod to which it is identical in construction and geometrical location. The effectiveness of the rods at elevated temperatures was more conveniently obtained by means of the temperature coefficient of reactivity.

Calibration by Period Measurement. This calibration was made with the core and reflector at 25°C and without circulation of the fuel. Starting with the reactor critical at low power, a rod was withdrawn approximately two inches, and the rise in power level over several decades was observed on a recording logarithmic count rate meter. A second rod was then inserted to stop the rise in power level returning the reactor to critical. In this manner, it was possible

to calibrate the entire rod in steps from completely inserted to completely withdrawn. Also, data was obtained simultaneously on the second rod.

The reactivity change brought about by moving the rod was computed from the reactor period using a theoretical inhour curve for the static reactor based on a delayed fraction of 0.755% and a photoneutron contribution of 0.033%.[14] In order to reduce the dependence of the experimental calibration on the value of prompt neutron generation time which had been calculated from theory, long periods, approximately 100 seconds, were used.

Calibration by Fuel Addition. The fuel concentration was increased in steps of the order of 0.1 gm U-235/Kg H_2O by adding concentrated uranyl sulfate solution. The change in concentration in the reactor was known very accurately from the quantity of fuel added and the inventory of water. At each concentration, the critical positions of the rods were noted along with fuel and reflector temperatures and reflector level. In this way, the increase in fuel concentration was correlated directly with the change in position of each rod. The reactivity change from the increase in fuel concentration was obtained from the concentration coefficient of reactivity, Figure 6. Usually a small correction for temperature change was required. The calibration data for the rods obtained both by period measurements and concentration change agree very well with each other and are shown in Figure 8 and 9.

Shim Rod Calibration at 200°C. After the temperature coefficient of the reactor was established by measurements of critical concentration over a range of core temperature, changes in temperature proved very useful in measuring reactivity. The shim rod was calibrated by this technique near 200°C which was close to the highest temperature feasible for low power calibrations. The reactor was

brought to criticality at 202°C by introducing building steam into the main fuel heat exchanger. The heat source was then turned off and while the reactor cooled, it was kept critical by inserting the shim rod. The fuel was of course circulating during this calibration in order to measure the temperature with the thermocouples on the circulating lines. The change in fuel temperature multiplied by the temperature coefficient of reactivity is then the reactivity controlled by the shim rod movement. The calibration of the shim rod at 200°C is also shown in Figure 9.

The experimental values obtained for the total reactivity controlled by the rods are listed in table VIII.

TABLE VIII

EFFECTIVENESS OF HRE RODS

$\frac{\Delta K_{EFF}}{K_{EFF}}$, PERCENT

Rod	25°C Experimental	25°C Calculated*	200°C Experimental	200°C Calculated*	250°C Calculated**
Control	0.33	0.77	0.41	1.1	-
Shim	.48	1.1	.61	1.4	4
Safety	.48	1.1	.61	1.4	4
All	1.29	3.0	1.63	3.9	8

*Calculated by P. M. Wood on the model of a curtain which is black to thermal neutrons

**Calculated by J. S. Stein by zero order perturbation method

Discussion. The excellent agreement in the results obtained by the two methods of rod calibration, reactor period and change in critical concentration, is indicative that the conversion from concentration to reactivity derived from theory is consistent with the values chosen for the effective delayed neutron and photo-gamma neutron contributions. The reliability of the reactivity-concentration conversion factor was also strongly supported by the close agreement between the measured critical concentration and that predicted from theory.

In Table VIII, a comparison is made between the observed and calculated values of the rods. It should be pointed out that since the bottom of any rods in its withdrawn position was no further than 10 inches removed from the core, one would expect, from the shape of the calibration curves, an additional 0.1 in Δk_{eff} percent for each rod if they could have been more completely withdrawn. The measured values of each rod at room temperature was approximately one-half percent lower in reactivity than calculated on the model of an absorbing curtain adjacent to the core tank, which is opaque to thermal neutrons. The discrepancy appears somewhat greater at elevated temperatures. An overestimate is made in assigning a value to the rods which is proportional to the solid angle subtended when the rods are inserted since the flux distribution is then distorted with its center shifted away from the plates. Another source of uncertainty in the calculations arises from the reactivity value of the core shell which is made of 347 stainless steel, 3/16 inch thick. For example, if this had been underestimated by one percent in Δk_{eff}, the safety rod would be overestimated by 0.2 percent in Δk_{eff}. Finally, it is apparent that the zero order perturbation method for calculating the value of the rods results in a very large over-estimate.

C. Reflector Calibration

Measurements at Room Temperature. As the fuel concentration in the core was increased in steps after the initial critical experiment, criticality was achieved near room temperature with all rods withdrawn at successively lower reflector levels. Data were obtained both with and without circulation of the fuel and were adjusted for the difference in reactivity. The height of the reflector was measured by means of a manometer connected directly to the pressure vessel as well as the installed liquid level transmitter. It was considered inadvisable at this stage to lower the reflector for these experiments more than two inches below the equator of the core in order to retain the only rapid shutdown devices available in the reactor: the dumping of the reflector and the dropping of rods into the reflector.

The data are listed in Table IX where at each reflector level, the change in concentration from the fully reflector reactor has been converted into a change in reactivity with corrections for changes in temperature and rod position. The treated data are plotted in Figure 10 where the points with the fuel circulating have been aligned with the static points by adding 0.60 percent k_{eff}. This difference arises from the loss of delayed neutrons on circulation and also from the difference in the datum for each set of points. In the region defined by the top and bottom of the core, there is a linear dependence of reactivity on reflector level, as was predicted. By virtue of the symmetry of the calibration curve, the total effectiveness of the reflector is twice the value from the reflector full position to the core equator. The resulting value of 6.5 percent k_{eff} is in good agreement with that predicted on the basis of extrapolation distance of 4 cm for the fast neutron group.

TABLE IX

REFLECTOR CALIBRATION AT ROOM TEMPERATURE
Fuel not Circulating

Datum: Shim, control and safety rods withdrawn, core temperature 25°C, concentration 24.88 gm U-235/Kg H_2O, reflector level 100 percent (full)

Fuel Concentration gm U-235/Kg H_2O	Reflector Level[1] Percent	Core Temperature °C	Rod Positions Inches Withdrawn Control[2]	Shim[3]	Δk_{eff}, percent From Temperature	From Rods	From Concentration	Total
24.92	100.0	25.3	8.3	10.9	-0.011	-0.025	0.060	0.02
25.28	80.0	25.2	0.0	4.0	- .008	- .574	.596	.01
25.28	70.0	25.2	0.0	6.0	- .008	- .466	.596	.12
25.03	66.3	23.8	12.6	9.0	- .046	- .070	.224	.20
25.28	66.0	25.2	0.0	9.1	- .008	- .311	.596	.28
25.28	60.5	25.4	12.7	11.0	- .015	0	.596	.58
25.48	60.5	25.6	0.7	11.0	- .023	- .300	.894	.57
25.48	58.7	25.4	12.7	10.8	- .015	0	.894	.88
25.48	58.5	25.1	10.7	11.0	- .004	- .012	.894	.88
25.63	56.4	24.3	11.4	11.0	+ .027	0	1.118	1.15
25.63	54.5	25.0	12.6	10.6	0	0	1.118	1.12
26.14	49.3	30.0	12.7	11.1	- .190	0	1.877	1.69
26.64	44.7	36.0	12.7	11.2	- .418	0	2.622	2.20
27.14	31.5	30.5	12.6	10.8	- .209	0	3.367	3.16
27.14	31.3	27.5	12.7	10.8	- .095	0	3.367	3.27
27.54	25.6	30.5	12.7	11.2	- .209	0	3.963	3.75

(1) Range of level indicator is 30 inches with zero corresponding to the bottom of the core tank.

(2) Fully withdrawn at 12.7 inches.

(3) Fully withdrawn at 11.2 inches.

UNCLASSIFIED

TABLE X

REFLECTOR CALIBRATION AT ROOM TEMPERATURE
Fuel Circulating

Datum: Shim inserted; control and safety rods withdrawn; core temperature 25°C; concentration 25.48 gm U-235/Kg H_2O

Fuel Concentration gm U-235/Kg H_2O	Reflector Level[1] Percent	Core Temperature °C	Rod Positions Inches Withdrawn Control[2]	Shim[3]	Δk_{eff}, percent From Temperature	From Rods	From Concentration	Total
25.48	73.7	25.5	12.7	0.0	-0.019	-0.419	0	-0.44
25.48	67.2	25.3	0.0	10.9	- .011	- .258	0	- .27
25.48	61.2	25.3	12.7	10.9	- .011	0	0	.01
25.63	57.8	25.8	11.2	11.1	- .030	0	.224	.19
26.14	52.0	30.5	12.7	11.1	- .209	0	.983	.77
26.14	51.5	29.2	12.7	11.1	- .160	0	.983	.82
26.64	48.2	36.6	12.7	11.2	- .441	0	1.728	1.29

(1) Range of level indicator is 30 inches with zero corresponding to the bottom of the core tank.

(2) Fully withdrawn at 12.7 inches.

(3) Fully withdrawn at 11.2 inches.

Reflector Calibration at Elevated Temperature. At 225°C, which was reasonably close to the design operating temperature of the reactor, the effectiveness of the reflector as a function of level was measured in two ways: by change in critical fuel concentration at constant temperature and by change in critical temperature at constant concentration. The temperature of the reflector was maintained at 200°C. Since the reactor pressure was kept at 1000 psig, it was not feasible to check the reflector level with a manometer; the level being determined solely by the differential pressure device with compensation for the change in density of the D_2O with temperature. Due to mechanical difficulties, the control rod remained permanently inserted during these measurements. Again, for safety considerations, the reflector level was not taken more than an inch or so below the core equator. The concentration of fuel was determined by gravimetric type analyses of the samples which were withdrawn as required in 20 ml aliquots. The data obtained primarily by change in concentration are presented in Table XI while that obtained from temperature data are in Table XII.

After the inherent stability and safety of the reactor had been demonstrated later in the experiments at high power, a calibration of the entire reflector was obtained by draining it completely. Because of the radioactivity of the fuel solution at this time, accurate analysis of the concentration were not feasible and the reflector was therefore calibrated by the change in critical temperature. As the reflector level was changed, the reactor automatically adjusted itself to delayed critical by heating or cooling as required. The reflector temperature was kept in the vicinity of 185°C; however, as will be described later, the temperature of the reflector has very little effect on reactivity. The data obtained here are also displayed in Table XII where the

TABLE XI

REFLECTOR CALIBRATION AT 220°C BY CONCENTRATION CHANGE

Reflector Temperature: 200°C
Shim and Safety Rods Withdrawn; Control Rod Inserted
$\partial k_{eff}/\partial T = -1.35 \times 10^{-3}/°C$ at 225°C

Fuel Concentration, gm U-235/Kg H_2O	Reflector Level, Percent	Core Temperature, °C	Δk_{eff}, percent		
			From Temperature	From Concentration	Total
37.74	100	228	-	-	Datum
37.80	92.5	230	-0.30	0.06	-0.24
37.68	100	226	.31	- .06	.25
37.01	51	224	.57	.25	.82
39.19	40	219	1.25	1.39	2.64
41.96	29.5	225	.45	3.91	4.36
37.91	58.5	220	1.08	.16	1.24

decrease in temperature has been converted to the equivalent Δk_{eff} by means of the appropriate temperature coefficient. It can be easily shown on the basis of the equivalent bare reactor model that to a good approximation, this coefficient is proportional to $(1/\rho)(\partial\rho/\partial T)$ when the concentration remains constant. Corrections were made to Δk_{eff} for minor changes in concentration and also for the presence of the inserted shim rod.

All the data obtained at the elevated temperatures were plotted in Figure 11 where again a linear relationship is indicated between reactivity and reflector level from the top to the bottom of the core. The data taken after high power operation are in very good agreement with the curve which was drawn through the earlier data and extended by reflection at the core equator. The effectiveness obtained in this manner for the entire reflector with control rod

TABLE XII

REFLECTOR CALIBRATION BY TEMPERATURE CHANGE
April 1953
Shim and Safety Rods Withdrawn, Control Rod Inserted
Fuel Concentration 37.7 gm U-235/Kg H_2O

Reflector Level % Full	Core Temperature °C	Condensate Holdup Kg	$\frac{\partial k_{eff}}{\partial T}$**, (-1) x 10^{-3}	Δk_{eff}, percent: Uncorrected	Corrected for Concentration	Corrected for Shim Rod and Concentration
100*	225	83	1.25	-	-	datum
80	224	83	1.25	-	-	0.13
69	223	83	1.25	-	-	.25
57	218	82	1.24	-	-	.87
50	209	82	1.20	-	-	1.92
40	201	82	1.14	-	-	2.74
39	201	82	1.14	-	-	2.74
February 6, 1954 Active Fuel Solution: 100 Kg						
91	224	92	1.25	0.75	0.08	0.08
0	165	92	.87	6.58	5.91	5.91
Drained	157	92	.84	7.25	6.58	7.18
Drained	157	92	.84	7.25	6.58	7.18
Drained	157	92	.84	7.25	6.58	7.18
0	165	92	.87	6.58	5.91	6.51
15	177	92	.92	5.51	4.84	5.44
30	195	94	1.03	3.89	3.89	4.19
45.3	210	94	1.14	2.36	2.36	2.36
61	224	94	1.25	.71	.71	.71
67	227	94	1.27	.36	.36	.36
92*	230	94	1.31	-	-	datum
93	224	92	1.25	.03	.03	.03
Drained	159	92	.84	6.44	6.44	7.04

This point is used as the datum.

** The ratio of this coefficient for a partially reflected configuration to that for the full reflector at the same concentration but at higher temperature is equal to the ratio of the values of

$$\frac{1}{\rho} \frac{\partial \rho}{\partial T}$$

where ρ is the density.

in is 7.7 percent in Δk_{eff}. The corresponding effectiveness when all rods are withdrawn would be 8.1 percent which agrees reasonably well with the value of 7.5 percent which is calculated as the reduction in reactivity in the bare reactor at 224°C when the fuel concentration is reduced from its critical value to the value which makes a fully reflected reactor critical at the same temperature. The comparison between theory and measurement can be made in a somewhat different manner by comparing the final critical temperature observed when the reflector was completely drained with the temperature predicted from the fuel concentration. From the calibrations performed on the HRE, the critical concentration at 224°C with a full reflector and with the control and shim rods inserted is 37.6 gm U-235 per Kg H_2O. At this concentration, calculations, using an extrapolation distance which is consistent with the 4 cm value at room temperature, indicate that the critical temperature when the reflector is removed should be 152°C as compared to the 157°C measured. By the same type of calculation, one predicts that the temperature reached on a shutdown from the 250°C operating temperature by dumping the reflector is 175°C.

D. Temperature Coefficient of Reactivity

The most important reactivity calibration in the HRE was the relationship between critical temperature and concentration of fuel since, for a reactor which is self-stabilizing, a change in reactivity is immediately reflected by a change in reactor temperature. Furthermore, from the rate of change of concentration with temperature can easily be obtained the temperature coefficient of reactivity which is an important parameter in the nuclear kinetics and safety of the reactor. The critical concentration was measured over the range of temperatures from 20°C to 230°C, the maximum attainable with external heating sources. The fuel concentration was reported in units of gm U-235/Kg H_2O which is invariant to the temperature of a sample of solution. Furthermore, the critical concentration in these units is practically independent of small variations in isotopic enrichment of the fuel. The reference condition of the reactor was: reflector full, all rods withdrawn, and the reflector temperature same as of the core. As it turned out, corrections for reflector temperature were negligibly small, a 40°C change in reflector being equivalent to only 1°C for the core.

The fuel temperature was measured by means of thermocouples attached to the main circulating lines and for the most part, the output was checked with a type K potentiometer. The reflector temperature was determined in a similar manner. To maintain fuel temperatures under approximately 105°C, it was necessary to circulate cooling water through the main heat exchanger in order to remove the heat input from the fuel circulating pump. Between 105°C and 200°C, the reactor was heated with plant steam in the main heat exchanger; and for higher temperatures, the steam source was an auxiliary electric boiler which

delivered 40 Kw of steam at 600 psig pressure.

Criticality Data from 20°C to 105°C. As in the case of the initial critical experiment, the measurements from 20°C to 105°C were made only on the high pressure fuel system which was isolated from the low pressure system. The methods of changing and measuring the fuel concentration were also the same. In this temperature range, criticality measurements were performed both with the fuel circulating and under static conditions in order to evaluate the change in the effective delayed neutron contribution due to circulation. The pressure was maintained at 100 psig with He for proper operation of the circulating pump.

The experiments were more difficult to perform with the main circulating pump off since the core temperature could not be directly measured. A procedure was therefore adopted whereby the temperature was measured while the pump was running, the pump was then stopped, and the reactor brought to delayed critical. The readings of the reactivity controls were noted as well as the time elapsed after turning off the pump. Due to heat losses, primarily to the reflector, the reactor temperature decreased. An empirical correction was determined for this cooling as a function of the initial temperature difference between core and reflector and the time elapsed. In Figure 12 is shown a cooling curve for an initial temperature difference of 4°C, with the core temperature inferred from the movement of the shim rod which was required to maintain the reactor critical. It should be pointed out that the correction for cooling which was applied to the static data never exceeded 3°C. The data are displayed in Table XIII where the various corrections are indicated.

The criticality data obtained with the fuel circulating are presented in Table XIV. All the data, both with the fuel static and circulating, for

TABLE XIII

CRITICAL FUEL CONCENTRATION BELOW 105°C WITHOUT CIRCULATION
REFLECTOR FULL: RODS WITHDRAWN

Measured Fuel Concentration, gm U-235/Kg H_2O	Correction for Rods		Corrected Fuel Concentration, gm U-235/Kg H_2O	Initial Fuel Temperature, °C	Reflector Temperature, °C	Time Pump was off, min	Temp. Correction, °C	Fuel Temp. when Critical °C
	Δk_{eff}, percent	Equiv. Change In Conc. gm U-235/Kg H_2O						
25.13	-0.24	-0.16	24.97	35.2	35.0	7	0	35.2
25.32	- .30	- .21	25.11	43	40	15	3	40
25.98	- .32	- .23	25.75	66.8	64	30	2.9	63.9
26.48	- .39	- .29	26.19	78.0	76	4	.4	77.6
26.97	- .54	- .40	26.57	92.8	88	5	1.2	91.6
26.97	- .35	- .26	26.71	94.0	91	5.2	.6	93.4
27.37	- .58	- .45	26.92	102.0	97	7	1.3	100.7
27.37	- .55	- .43	26.94	101.7	100	7	.5	101.2
27.37	- .36	- .28	27.09	104.2	100	3.5	.7	103.5
27.37	- .36	- .28	27.09	104.9	101	6.5	.9	104.0

UNCLASSIFIED

temperatures under 105°C are shown in Figure 13 where curves were drawn through the data for the purpose of estimating the slopes. A loss of reactivity is indicated upon circulation of the fuel solution, equivalent to 0.12 gm U-235 per Kg H_2O at 30°C increasing to 0.18 gm U-235/Kg H_2O at 100°C. The corresponding reactivities in Δk_{eff} are 0.18 percent at 30°C and 0.23 percent at 100°C. The estimated loss in delayed neutron fraction had been predicted as 0.20 percent: 0.15 percent loss due to emission of the neutron in the external circuit[15] and 0.05 percent due to the mixing of the precursors throughout the core.

Criticality Data from 100°C to 250°C. For the experiments in this temperature range, the fuel system was connected together as intended for normal operation, permitting circulation between high and low pressure components at one gpm by means of the pulsafeeder type pump. The fuel concentration was changed as needed by changing the inventory of condensate in the concentration control system. For each critical point in the range from 100°C to 217°C, two samples of solution were withdrawn from the high pressure circulating stream by means of the sample bombs of 50 ml capacity. However, for the data above 217°C, the temporary sampling rig was replaced by a remote sampler for radioactive solution and as mentioned earlier, the error in determining the concentration increased. In order to reach the temperature of 240°C and higher, the reactor was heated by raising the power level to 50 Kw, and because of the radioactivity produced in the fuel solution, the concentration was inferred primarily from considerations of fuel and condensate inventory.

The data are presented in Table XIII while in Figure 14 are plotted all the data obtained from 20°C to 250°C with the fuel circulating. The curve calculated by the Feynman-Welton approximation (Appendix I) is also shown for comparison.

TABLE XIV

CRITICAL FUEL CONCENTRATIONS WITH CIRCULATION

Reflector Full; Rods Withdrawn
High Pressure System Alone

Measured Fuel Conc. gm U-235/Kg H_2O	Reactivity Corrections: Rods Δk_{eff} (-) %	Pressure Δk_{eff} (+) %	Reflector Δk_{eff} (-) %	Equivalent Change in Conc. gm U-235/Kg H_2O	Corrected Fuel Conc. gm U-235/Kg H_2O	Core Temp. °C	Reflector Temp. °C	Fuel Pressure psig
25.13	0.59	0	0	0.39	24.73	22	25	100
25.13	.45	0	0	.30	24.82	26	25	100
25.13	.40	0	0	.27	24.85	27	25	100
25.13	.34	0	0	.23	24.90	26	25	100
25.13	.27	0	0	.18	24.95	30	25	100
25.13	.11	0	0	.08	25.05	33	25	100
25.13	.04	0	0	.03	25.10	34	25	100
25.13	0	0	0	0	25.13	37	25	100
25.32	0	0	0	0	25.32	43	25	100
25.47	0	0	0	0	25.47	49	25	100
25.98	.78	0	0	.55	25.44	50	25	100
26.48	.76	0	0	.55	55.93	67	25	100
25.98	0	0	0	0	25.98	67	25	100
26.48	.20	0	0	.15	26.33	79	25	100
26.48	.11	0	0	.08	26.40	80	79	100
26.97	.67	0	0	.49	26.48	82	79	120
26.48	0	0	0	0	26.48	83	79	120
26.97	.22	0	0	.17	26.81	92	87	260
26.97	.16	0	0	.12	26.86	93	92	100
26.97	0	0	0	0	26.97	96	94	120
27.37	.41	0	0	.31	27.06	100	95	300
27.37	.37	0	0	.28	27.09	101	95	300
27.37	.26	0	0	.20	27.17	102	100	300
27.37	.05	0	0	.04	27.33	104	100	120
27.37	.02	0	0	.02	27.36	105	102	120
27.37	0	0	0	0	27.37	105	104	120
25.13	.40	0	0	.27	24.85	27	25	100
25.13	.36	0	0	.24	24.89	28	25	100

UNCLASSIFIED

TABLE XIV (Cont'd)

Measured Fuel Conc. gm U-235/Kg H_2O	Reactivity Corrections: Rods Δk_{eff} (-) %	Pressure Δk_{eff} (+) %	Reflector Δk_{eff} (-) %	Equivalent Change in Conc. gm U-235/Kg H_2O	Corrected Fuel Conc. gm U-235/Kg H_2O	Core Temp. °C	Reflector Temp. °C	Fuel Pressure psig
25.13	.31	0	0	.21	24.92	29	25	100
25.13	.30	0	0	.20	24.92	29	25	100
25.13	.29	0	0	.19	24.93	30	25	100
25.13	.16	0	0	.11	25.02	32	25	100
25.13	.06	0	0	.04	25.08	33	25	100
25.13	.03	0	0	.02	25.11	35	25	100
25.13	.03	0	0	.02	25.11	35	25	100
25.98	0	0	0	0	25.98	67	64	100
25.98	0	0	0	0	25.98	67	65	100
26.48	.76	0	0	.55	25.94	68	60	100
26.48	.13	0	0	.10	26.38	80	79	120
26.98	0	0	0	0	26.97	96	94	120
27.37	.42	0	0	.32	27.05	99	93	100
27.37	.42	0	0	.32	27.05	99	93	100
27.37	.42	0	0	.32	27.05	99	94	100
27.37	.40	0	0	.30	27.07	100	95	100
27.37	.39	0	0	.30	27.07	100	95	100
27.37	.34	0	0	.26	27.11	100	95	100
27.37	.34	0	0	.26	27.11	101	95	100
27.37	.31	0	0	.24	27.14	102	100	100
27.37	.30	0	0	.23	27.14	102	100	100
27.37	.35	0	0	.27	27.10	102	98	600
27.37	.27	0	0	.21	27.16	103	100	910
			High-and Low-Pressure Systems Connected Together					
27.50	.57	0.06	0	.39	27.11	96	89	520
27.63	.72	.06	0	.50	27.13	98	90	440
27.63	.69	.06	0	.48	27.15	99	92	460
27.68	.70	.09	0	.47	27.22	100	93	600
27.68	.66	.09	0	.44	27.24	101	93	600
27.63	.49	.06	0	.33	27.30	103	94	420

UNCLASSIFIED

TABLE XIV (Cont'd)

Measured Fuel Conc. gm U-235/Kg H_2O	Reactivity Corrections: Rods Δk_{eff} (-) %	Pressure Δk_{eff} (+) %	Reflector Δk_{eff} (-) %	Equivalent Change in Conc. gm U-235/Kg H_2O	Corrected Fuel Conc. gm U-235/Kg H_2O	Core Temp. °C	Reflector Temp. °C	Fuel Pressure psig
			High-and-Low Pressure Systems Connected Together					
27.63	.38	.06	0	.24	27.39	103	95	430
27.41	.04	.06	0	.20	27.43	105	100	520
22.41	.01	.06	0	.04	27.45	106	101	530
28.52	.25	.07	0	.14	28.38	120	138	460
28.43	.06	.08	0	.01	28.44	126	123	450
29.46	.15	.09	0	.06	29.41	144	145	380
29.46	.09	.09	0	0	29.46	145	147	440
30.66	.34	.10	0	.22	30.44	164	165	440
32.07	.56	.10	0	.43	31.64	177	184	500
33.00	.01	.28	0	.27	32.27	198	178	1000
33.45	.24	.14	0	.10	33.35	201	176	560
33.43	.10	.14	0	.04	33.39	201	186	540
33.43	.07	.15	0	.08	33.35	201	186	560
33.43	.07	.15	0	.07	33.36	201	186	560
33.52	.02	.14	0	.13	33.58	202	201	580
33.45	.02	.14	0	.13	33.58	202	201	550
33.45	.01	.14	0	.13	33.58	202	200	580
33.43	.45	.11	0	.34	35.09	217	203	460
33.43	.30	.11	0	.19	35.24	217	200	450
33.43	.34	.11	0	.23	35.21	217	203	460
28.12	.33	.06	.54	.66	27.46	102	94	500
24.37	.42	.06	.01	.43	33.94	204	198	500
37.96	.42	.06	.22	.68	37.38	222	200	500
37.96	.42	.06	.22	.68	37.38	221	200	500
37.80	.42	.06	0	.46	37.34	229	207	500
37.62	.42	.06	0	.45	37.17	225	203	500
37.62	.42	.06	0	.45	37.17	225	200	500
39.42	.42	.38	.11	.18	39.24	244	190	1000

UNCLASSIFIED

The agreement with experiment is remarkably good indicating the adequacy of two-group diffusion theory and the reactor constants for predicting the critical conditions for aqueous homogeneous reactors where fissions occur primarily at thermal neutron energies.

Temperature Coefficient of Reactivity. The temperature coefficient of reactivity was obtained at intervals of 25°C from the rate of change of fuel concentration, C, with critical temperature, T, in Figure 14. The product of $\partial C/\partial T$ and $\partial k_{eff}/\partial C$ appropriate to each temperature gave $\partial k_{eff}/\partial T$. In Figure 15 are shown the measured coefficients along with the theoretical predictions obtained by differentiating the two-group criticality equation for the equivalent bare sphere (Appendix III). It is to be recalled that the values obtained by this calculation are very close to those obtained by the method of performing independent criticality calculations at two temperatures a few degrees apart. The agreement with the measured values of the temperature coefficient is within the experimental error.

Reflector Temperature Coefficient of Reactivity. To evaluate the reactivity coefficient associated with the reflector temperature, criticality data were taken with the fuel concentration held constant and the core temperature maintained at 200°C while the reflector temperature was varied from 150°C to 201°C. The resulting reactivity changes were measured by means of the movement of the shim rod which was necessary to keep the reactor critical. The results are shown in Figure 16 where the slope of the line drawn through the data gives minus 2.5×10^{-5} $k_{eff}/°C$ as the temperature coefficient for the reflector. A similar experiment at 120°C core temperature gave the value there as minus 1.4×10^{-5}.

The value of minus 1.5 x $10^{-4}/^{o}C$ had been calculated[16] for the coefficient at 175°C, which is six times the value measured at 200°C. The calculations were then refined to take into account the change in absorption cross-section of the core tank with reflector temperature and also the change in dimension of core tank and pressure vessel for thermal expansion. The net result was to lower the theoretical value to only minus 1.2 x $10^{-4}/^{o}C$. The discrepancy most likely arises from the uncertainty in the ratio of the fast diffusion constant in light to heavy water; this quantity being somewhat arbitrary in two-group diffusion theory.

E. Pressure Coefficient of Reactivity

The effect of changing the pressure in the high pressure fuel and reflector systems on the multiplication constant of the reactor was measured at 23.5°C with the high pressure loop isolated from the balance of the reactor system. The experiment was performed with both the fuel and reflector circulating pumps off. The pressure in the core was regulated with helium supplied to the top of the pressurizer while the reflector pressure was controlled by the regular pressurization system. The pressures in the core and reflector vessel were varied together from 0 to 1000 psig and the reactor kept critical by adjusting the control rod. Measurements were also made with the reflector pressure reduced to 100 psig and the core pressure maintained at 1000 psig. In both cases, the effect of pressure was to compress the water; but the important difference between the two sets of measurements is the stretching of the core tank.

The data are listed in Table XIV. The control rod movement was converted to reactivity change by means of the control rod calibration curve and the resulting relationship between pressure and reactivity is shown in Figure 17. The

slope of the curve gives the value of the pressure coefficient of reactivity at 23.5°C as 0.16 percent k_{eff}/1000 psi, with core and reflector at the same pressure. The effect of a pressure differential of 880 psi across the core tank is 0.18 percent Δk_{eff}, which extrapolates to give 0.20 percent for 1000 psi. These measurements are in excellent agreement with the values calculated by means of the two-group diffusion equation for the equivalent bare sphere.

TABLE XV

EFFECT OF PRESSURE ON REACTIVITY

Reflector full: Shim rod inserted; Safety rod withdrawn

Fuel Concentration: 25.28 gm U^{235}/Kg H_2O
Temperature: 23.5°C

Core Pressure psig	Reflector Pressure psig	Control Rod Position Inches Withdrawn	Reactivity % k_{eff}
0	100	4.9	-0.01
0	100	4.7	Datum
170	267	3.6	.04
0	150	4.5	.01
180	207	3.7	.04
390	435	3.0	.07
595	575	21	.10
780	810	1.5	.13
1000	1000	0.8	.15
980	100	0	.18
800	100	0.9	.15
0	100	4.7	0

F. Inhour Experiments

The purpose of these experiments was to establish the relationship between excess reactivity and the stable period of the resulting exponential rise in power level. At low power where there is no appreciable fission heating, this relationship for small reactivity increases depends primarily on the delayed neutrons in the reactor core. There is also the small contribution, 0.023 percent, of the photoneutrons generated in the D_2O reflector[14] from gamma photons emitted by the fission products in the core. On circulation, there is a decrease in both the effective delayed neutrons and photoneutrons owing to the emission of neutrons and gammas in the external system.[15] There is the additional loss in effectiveness of 0.04 percent from the net transport of delayed neutron emitters in the core from regions of higher to lower nuclear importance. The loss of precursors of the delayed neutrons from the fuel solution for chemical reasons, e. g. iodine, which could be influenced by changes in temperature and by gas generation at higher power levels was a possibility.

The inhour experiments are performed under both static and circulating conditions and at several temperatures: 25°, 100°, and 200°C. After it was established that the reactor was in a steady critical state, the control or shim rod was withdrawn to add reactivity. The rise in power level was recorded on a logarithmic count-rate meter connected to a fission chamber enabling one to establish the period from the straight portion of the curve. The measurements in general were rather difficult to make since, in a reactor with a temperature coefficient of reactivity of the order of 0.1 percent k_{eff} per degree Centigrade, a small change in temperature would invalidate the measurements. The only experiments accepted were those in which it was possible to return the reactor

to critical after the rise in power by inserting the rods to their previous positions. The reactivity which had been introduced by the rods was determined from their calibration in terms of fuel concentration. Periods as short as eight seconds were recorded corresponding to a maximum reactivity increase of 0.28 percent in k_{eff}. With the fuel circulating at 120 gpm, the residence times in the high pressure system is 6.6 sec in the core and 2.1 sec outside.

The data obtained at room temperature without circulation of the fuel are listed in Table XVI and all the data with circulation are in Table XVII.

TABLE XVI

STATIC INHOUR DATA AT 28°C

Reflector Full; Fuel Concentration: 25.3 gm U^{235}/Kg H_2O

Reactivity, percent	Period sec
0.077	102
.200	26
.065	129
.224	19.7
.213	19.3
.284	13.5
.072	110
.130	47.2
.105	63.2
.050	251
.058	155

TABLE XVII

INHOUR DATA WITH CIRCULATION OF FUEL

Fuel Temperature, °C	Reactivity, Percent	Period, Sec
27	0.077	64.4
27	.054	132
27	.058	95.8
27	.065	94.7
27	.066	100
27	.061	94.7
26	.044	113
27	.158	19.5
29	.024	298
30	.065	80.8
30	.030	189
30	.019	311
30	.046	138
30	.023	297
26	.126	21.1
26	.109	28.5
25	.180	12.1
100	.071	81.3
100	.135	22.1
101	.177	12.5
100	.043	103
102	.043	95.4
102	.022	214
100	.038	126
101	.030	149
99	.020	180
200	.105	29.9
200	.196	9.4
200	.196	11.3
200	.068	72.7
202	.175	9.5
202	.078	38.8
202	.050	57.5
202	.041	174
200	.048	54.2
202	.131	19.1

All the experimental inhour curves are plotted in Figure 18 along with the theoretical curves based on an effective delayed neutron fraction of 7.55×10^{-3} and a photoneutron contribution of 0.23×10^{-3} or combined fraction of 7.78×10^{-3} for the static condition. The very good agreement for the static case supports the above estimates and is not surprising in view of the earlier observation concerning the agreement between the calibration data of the rods by period and concentration measurements. There is no significant difference in the inhour data for the circulating reactor obtained at the three temperatures, indicating that the relative quantity of delayed neutron precursors remains essentially constant in the temperature range from 25° to 200°C. The experimental data however does fall somewhat below the theoretical curve which would indicate that the effective value of the delayed neutron fraction with circulation is somewhat smaller than the calculated value of 5.87×10^{-3}. This is supported by the criticality data on starting and stopping the pump which, it will be recalled, indicated that the change in reactivity, which is numerically equal to the change in effective delayed neutron fraction, was between 1.8 and 2.3×10^{-3} k_{eff} as compared to the calculated value of 1.7×10^{-3}.

V. SUMMARY AND CONCLUSIONS

The HRE was first made critical on April 15, 1952 in a static condition at room temperature with the reactor fully reflected by D_2O, with rods withdrawn, and with a fuel concentration of 24.8 gm U-235/Kg H_2O. Shortly thereafter, criticality was reached with the fuel circulating, demonstrating for the first time a nuclear chain reaction in a reactor through which a fluid fuel circulates and where there is an appreciable loss of delayed neutrons in the external circuit. No unusual problems came to light in the course of this demonstration aside from the loss and recovery of reactivity on starting and stopping the pump.

It proved feasible to measure all the important reactivity constants and coefficients for the reactor and these are summarized as follows:

1. Critical Concentration. The critical fuel concentration increased with temperature as shown in Figure 14 from 24.8 gm U-235/Kg H_2O at 20°C to 38.9 gm U-235/Kg H_2O at 235°C. The experimentally determined concentrations follow the theoretical curve very well but are about two percent lower.

2. Temperature Coefficient of Reactivity. The measured values of the temperature coefficient are in good agreement with that calculated by differentiating the two-group criticality equation for the equivalent bare sphere. The coefficient is negative and its magnitude increases with temperature; 0.37×10^{-3} $k_{eff}/°C$ at 20°C and 1.15×10^{-3} $k_{eff}/°C$ at 220°C.

3. Reflector Effectiveness. The value of the reflector in Δk_{eff} was measured as only 6.5 percent at room temperature and 7.5 percent at 225°C. These values were predicted when an extrapolation distance of 4 cm was used in the criticality calculation for the unreflected reactor at 20°C. The earliest estimates without any extrapolation distance gave 25 percent for the effectiveness of the reflector at 250°C. Whereas on this erroneous basis, a shutdown of the reactor

at 250°C by draining the reflector would have insured a sub-critical state should the reactor cool to room temperature, the later results, supported by experiment, indicate that the reactor would again become critical while unreflected if cooled to 170°C. It was demonstrated in one experiment which started at 225°C with the reflector filled and the control and shim rods inserted, that the reactor became critical at 157°C after the reflector was dumped. This would imply that in order to maintain the reactor sub-critical after the reflector is dumped, one of the following courses of action were necessary: diluting the fuel, keeping the temperature above the critical temperature, admitting house steam into the heat exchanger readily permits holding 200°C which is more than adequate; or finally, dumping the fuel from the core.

4. Effectiveness of Rods. At room temperature the value of the control rod in Δk_{eff} was 0.4 percent and of the shim and safety rods, 0.5 percent each. At 200°C, the value of the rods was increased by about 20 percent. The calculations by perturbation methods overestimated the value of the rods by a factor of 5. The method where the rods are considered to be a portion of a curtain about the core, which is a perfect absorber of the thermal neutrons but is transparent to fast neutrons, gave 2.9 percent as the value for all rods together at room temperature as compared to the observed value of 1.4 percent.

5. Effective Delayed Neutron Fraction. It was shown that under static conditions, the value of 0.755 percent for the ordinary delayed neutron fraction and 0.023 percent for the delayed photoneutrons gave rod calibrations and inhour relationships which were consistent with the calibration of the rods by change in critical concentration. With the fuel circulating at 120 gpm--corresponding to a residence time of 6.6 sec inside the core and 2.1 sec outside--it had been

predicted that the total effective delayed neutron fraction would decrease by 0.20 percent. This was confirmed by direct measurements of the change in reactivity on starting and stopping the circulating pump. The observed inhour relationship with circulation agreed well with the predicted curve although there are indications that the best fit to experimental data would require a decrease in the effective delayed neutron fraction of 0.25 percent. In any case, there still remained an effective delayed neutron fraction of at least 0.50 percent which, together with the sizeable negative temperature coefficient of reactivity, was more than adequate to insure stable operation of the reactor.

APPENDIX I

PURITY OF FUEL SOLUTION

The fuel solution was analyzed spectrographically for impurities, and the nuclear poisoning from the impurities was compared to that of the sulfate ion associated with the fuel as UO_2SO_4. In Table XVIII are calculated, for a typical batch of fuel of 29.24 weight percent uranium, the values of the macroscopic absorption cross-section for thermal neutrons for each element. The total macroscopic cross-section of the impurities is 17.07×10^{-6}/cm as compared to the value of 351.6×10^{-6} for the sulfate ion in the solution; the ratio of the two is only 0.05.

TABLE XVIII

CHEMICAL IMPURITIES IN FUEL

Wt. Percent Uranium = 29.24
Macroscopic Sulfur Capture Cross-Section = 351.6 x 10^{-6} cm^{-1}

Element	Atomic Wt.	Absorption Cross-Section, barns (20°C)	Concentration, ppm	$\Sigma_a \times 10^{+6}$, cm^{-1}
Al	27	.22	.6	.0029
As	75	4.1	6.6*	.217
Au	197	96	.6*	.176
B	10.8	718	.3	12.00
Ba	137	1.1	1.3*	.0063
Be	9.0	.01	.006*	.00004
Bi	209	.015	.3*	.00001
Ca	40	.5	3	.0226
Cd	112	3170	.06*	1.022
Co	59	36	.3*	.110
Cr	52	2.9	1	.0336
Cu	63.6	3.6	2	.0680
Fe	55.9	2.5	8	.216
Ga	69.7	2.8	.3*	.073
Ge	72.6	2.2	.13*	.0024
Hg	201	349	1.3*	1.360
In	115	191	.6*	.602
Li	7	65	.06*	.335
Mg	24	.06	1	.0015
Mn	55	12.8	.3*	.0420
Mo	96	2.6	2.6	.0424
Na	23	.5	.5	.0066
Ni	59	4.7	1	.0480
P	31	.2	33*	.128
Pb	207	19	.3	.0166
Pd	107	6.6	.3*	.0111
Sb	122	5.3	1.3*	.0340
Si	28	.1	8	.0172
Sn	119	.58	.3*	.0009
Sr	88	1.3	6.6*	.0587
Ti	48	5.3	6.6	.439
Tl	204	3.27	1.3*	.0125
V	51	5	.016*	.0010
Zn	65	.9	3*	.0250

Σ_a(Total) = 17.07 x 10^{-6} cm^{-1}

* Concentration reported as less than value given. For calculation purposes, this upper limit was used.

APPENDIX II

Calculations of HRE Criticality by P. M. Wood

Subsequent to the calculations made by Stein and Welton and just prior to the initial criticality of the HRE, calculations using new constants were performed for predicting the critical concentration of the bare and reflected reactor. The essential difference in the calculation of the bare reactor is the choice of an appreciable extrapolation distance which is supported by an analysis of experimental criticality data and which leads to an estimated reflector effectiveness substantially smaller than previous estimates. Separate extrapolation distances were used for each neutron group. For the reflected reactor, the results are very similar.

Reactor Constants (at 20°C unless otherwise indicated)

Constants for H_2O

$\sigma_a(H_2O) = 0.64$ b/molecule

Age, $\tau = 33$ cm^2

Square of diffusion length, $L_o^2 = 7.068$ cm^2

$\Sigma_a(H_2O) = 0.02136$ cm^{-1}

Fast diffusion constant, $D_f = 1.9$ cm

Slow diffusion constant, $D_s = 0.1614$ cm

Density, $\rho(20°C) = 0.9982$ gm/cm^3

$\rho(250°C) = 0.7940$ gm/cm^3

Scattering cross-section, $\sigma_s(20°C) = 52.2$ b/H atom

$\sigma_s(250°C) = 43.2$ b/H atom

Constants for D_2O

$\sigma_a(D_2O) = 0.00182$ b/molecule

$\Sigma_a(D_2O) = 6.02 \times 10^{-5}$ cm^{-1} at 20°C

$\tau = 120$ cm^2 at 20°C

$L_o^2 = 1.513 \times 10^4$ cm^2 at 20°C

$\rho(20°C) = 1.103$ gm/cm^3

$\rho(175°C) = 0.9775$ gm/cm^3

$\sigma_s(20°C) = 14.5$ b/molecule

$\sigma_s(175°C) = 13.8$ b/molecule

Constants for Stainless Steel (347) at 20°C

$\Sigma_a = 0.24\ cm^{-1}$ $L_o^2 = 1.0\ cm^2$

Constants for Uranium at 20°C

$\sigma_f(25) = 546$ b $\nu\ (25) = 2.5$

$\sigma_a(25) = 644$ b η (fuel) = 2.119 (93.4% U-235)

$\sigma_a(28) = 2.9$ b Resonance escape probability M 0.996

The value for the fast diffusion constant is obtained as follows: let τ be the experimentally determined square of the slowing down length and Σ_f be the macroscopic cross-section for the removal of neutrons from the fast group by thermalization. Then $D_f = \tau\Sigma_f$. Now the quantity Σ_f is the ratio of the average fast scattering macroscopic cross-section to the average number of collisions for thermalizing a fission neutron. The fast scattering cross section is averaged over the asymptotic energy distribution of the flux given by $\Phi(E)dE = \frac{dE}{\sigma_s(E)\ E}$. This method of obtaining D_f is preferred for a hydrogeneous moderator as it uses the experimental "age" τ and thereby eliminates some of the errors in the Fermi "age" model which are inherent in the alternative method of averaging the transport mean free path for the fast group.

Unreflected HRE

In order to check the constants and extrapolation distance to be used for calculating the HRE criticality, an analysis was made of the criticality experiments by Beck, Callihan, et al on bare cylinders.[16] The fuel was a solution of 93 per cent enriched UO_2F_2 in light water, and the cylinders were made of stainless steel type 347, 1/16 inch thick. Ordinary two-group diffusion theory was used with an extrapolation distance of 0.71 λ_{tr} where the value of λ_{tr} for each neutron group is three times the appropriate diffusion constant.

Analysis of Criticality Data for Unreflected Cylinders

Reactor Diameter, inches	Reactor Height, Cm	Experimental Critical Concentration, gm U-235/Kg H_2O	Theoretical Critical Concentration gm U-235/Kg H_2O
20	26.7	34.3	35.36
20	20.5	52.2	50.57
15	41.7	34.3	35.18
15	27.0	52.2	50.57
12	48.9	52.2	49.30
12	30.3	80.5	81.08*
10	46.6	114.0	106.55*

*Hydrogen displacement taken into account.

Additional calculations were made for comparison in the case of the cylinder of 15" diameter and 41.7 cm height which had a critical concentration of 34.3, with the following changes in constants:

1. Using the same extrapolation distances as in the preceeding calculations but taking $\sigma_a(20^oC)$ of H_2O as 0.69 molecule, the critical concentration is 37.4 gm(25)/Kg H_2O.
2. Using $\sigma_a(H_2O)$ = 0.64 b/molecule but taking D_f = 1.143 cm from MonP-402 instead of 1.9 cm, the critical concentration is 42.8 gm 25/Kg H_2O.

It is evident that the values of 0.64 b for $\sigma_a(H_2O)$ and 1.9 cm for D_f, with which the critical concentration of 35.2 gm U 25/Kg H_2O was obtained, give the best agreement with experiment. The critical concentration for the bare HRE was then calculated using these constants and extrapolation distances. The

effect of the 3/16" stainless steel core shell was included as a reflector savings. The results as a function of temperature are shown in Figure 20.

The effect of the 3-inch thick steel pressure shell was computed by first calculating the return of neutrons by the shell to the core and applying an effectiveness factor of 1/5 for neutrons returned by the shell. This effect lowered the critical concentration by 0.83 gm 25/Kg or 0.9% k_{eff}, the decrease being directly proportional to the effectiveness factor assumed. The critical concentration of the unreflected reactor corrected for this effect is also shown in Figure 20.

Reflected HRE

Using the method of Feynman and Welton,[8] calculations were made for the HRE reflected with D_2O for the temperature range from 20° to 250°C. The effect of the 3/16" stainless steel core shell is 2% k_{eff} at 20°C and 3.2% k_{eff} at 250°C. The results are plotted in Figure 14 where the experimental results are also shown.

A plot of k_{eff} as a function of fuel concentration is given in Figure 19 for the HRE, bare and reflected, at 20°C and 250°C core temperatures. This plot shows that the effectiveness of the reflector is:

7.5% k_{eff} at 20°C core and reflector

11.2% k_{eff} at 250°C core 175°C reflector

The reactor core, containing 41.3 gm 25/Kg--the critical concentration for the D_2O reflected reactor at 250°C core temperature and 175°C reflector temperature--will be critical, with the reflector completely drained, in the neighborhood of 170°C.

APPENDIX III

Calculation of Temperature Coefficient of Reactivity

The temperature coefficient of reactivity of a bare reactor can be obtained directly by differentiation of the two-group criticality equation,

$$(1) \qquad k_{eff} = \frac{\eta f P}{(1 + L^2B^2)(1 + \tau B^2)}$$

where

η = number of neutrons obtained for each neutron absorbed in the fuel

P = resonance escape probability

f = thermal utilization;

$$f = \frac{\sum(\text{fuel})}{\sum(\text{fuel}) + \sum(\text{moderator})}$$

τ = Fermi age

L = thermal diffusion length in fuel solution,

$$L^2 = \frac{D_s}{\sum(\text{fuel}) + \sum(\text{moderator})}$$

D_s = diffusion constant for thermal neutrons

B^2 = buckling

For the case where P is essentially unity, one obtains on differentiation,

$$(2) \qquad \frac{1}{k_{eff}} \frac{\partial k_{eff}}{\partial T} = \frac{1}{f}\frac{\partial f}{\partial T} - \frac{B^2}{1 + L^2B^2}\frac{\partial L^2}{\partial T} - \frac{B^2}{1 + \tau B^2}\frac{\partial \tau}{\partial T}$$

Now by definition

$$(3) \qquad \frac{1}{f} = 1 + \frac{N_H \sigma_H}{N_U \sigma_U}$$

where σ is the microscopic absorption cross-section and N is the atomic density.

By differentiation,

$$(4) \quad \frac{1}{f} \frac{\partial f}{\partial T} = (1 - f) \quad \frac{1}{\sigma_U} \frac{\partial \sigma_U}{\partial T} - \frac{1}{\sigma_H} \frac{\partial \sigma_H}{\partial T} \quad .$$

Since $\sigma_H \alpha T^{-0.5}$, we have

$$(5) \quad \frac{1}{\sigma_H} \frac{\partial \sigma_H}{\partial T} = - \frac{0.500}{T}$$

From the observed energy dependence of the thermal absorption cross-section of U-235,

$\sigma_U \alpha T^{-0.614}$ and therefore

$$(6) \quad \frac{1}{\sigma_U} \frac{\partial \sigma_U}{\partial T} = - \frac{0.614}{T}$$

We now obtain

$$(7) \quad \frac{1}{f} \frac{\partial f}{\partial T} = - \frac{0.114}{T} (1 - f)$$

$$= - \frac{0.114}{T} \frac{\eta - k_\infty}{\eta}$$

The dependence of τ on the temperature is only through the square of the density, ρ:

$$(8) \quad \frac{1}{\tau} \frac{\partial \tau}{\partial T} = - \frac{2}{\rho} \frac{\partial \rho}{\partial T}$$

In the case of L^2, the temperature dependence is not only through the density but also through the thermal scattering cross-section of light water ($\sigma_s \alpha \ell^{-1.12 \times 10^{-3} T}$) and the absorption cross-sections of water and uranium. If L_o is the thermal diffusion length in plain water,

$$(9) \quad L^2 = L_o^2 (1 - f)$$

$$(10) \quad \frac{1}{L^2} \frac{\partial L^2}{\partial T} = \frac{1}{L_o^2} \frac{\partial L_o^2}{\partial T} - \frac{1}{(1 - f)} \frac{\partial f}{\partial T}$$

Now,

$$(11) \quad \frac{1}{L_o^2} \frac{\partial L_o^2}{\partial T} = - \frac{2}{\rho} \frac{\partial \rho}{\partial T} + \frac{0.5}{T} + 1.12 \times 10^{-3}$$

and from (7)

$$(12) \quad \frac{1}{(1 - f)} \frac{\partial f}{\partial T} = - \frac{0.114}{T} f = - \frac{0.114}{T} \frac{k_\infty}{\eta}$$

On substituting (11) and (12) into (10), we obtain

$$(13) \quad \frac{1}{L^2} \frac{\partial L^2}{\partial T} = 1.12 \times 10^{-3} - \frac{2}{\rho} \frac{\partial \rho}{\partial T} + \left(0.5 + 0.114 \frac{k_\infty}{\eta}\right) \frac{1}{T}$$

Finally,

$$(14) \quad \frac{\partial k_{eff}}{\partial T} = - k_{eff} \frac{0.114}{T} \frac{\eta - k_\infty}{\eta} - \frac{L^2 B^2}{1 + L^2 B^2} \left[1.12 \times 10^{-3} + \frac{2}{\rho} \left| \frac{\partial \rho}{\partial T} \right| + 0.5 + 0.114 \frac{k_\infty}{\eta} \frac{1}{T} \right] - \frac{2 \gamma B^2}{1 + \gamma B^2} \frac{1}{\rho} \left| \frac{\partial \rho}{\partial T} \right|$$

Unclassified
Dwg. D-9065 A

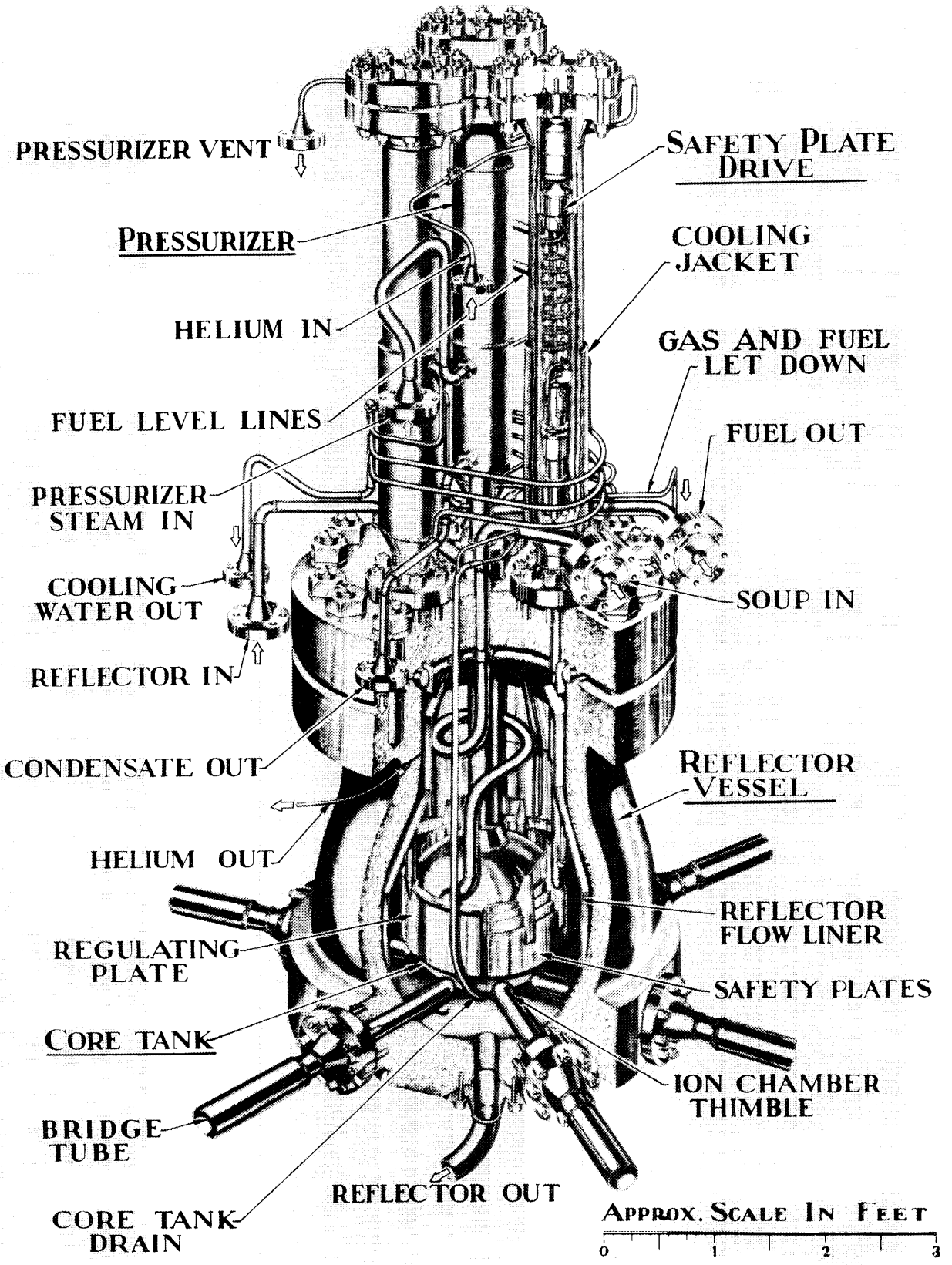

Fig. 1. Reactor Vessel.

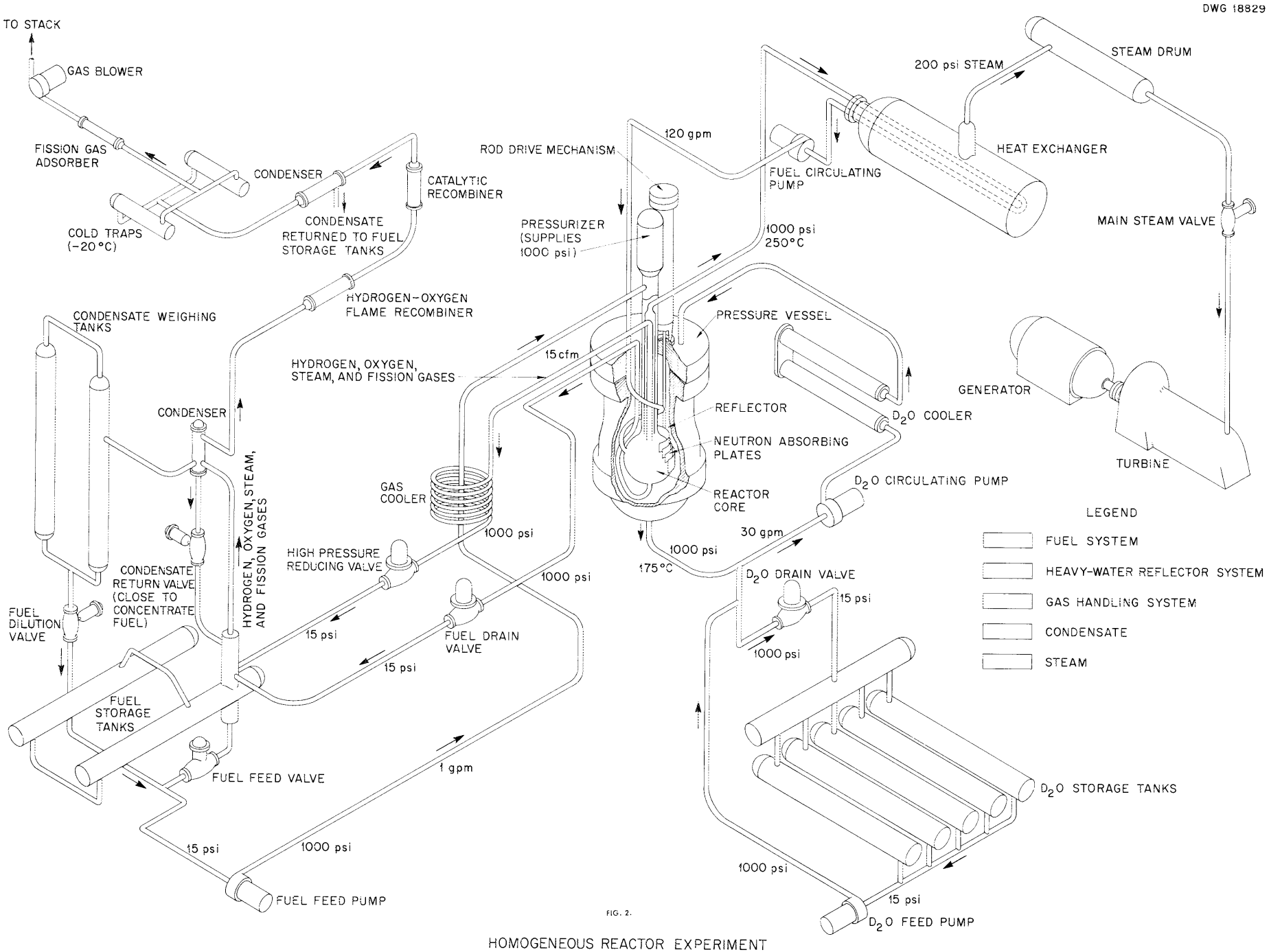

FIG. 2.

HOMOGENEOUS REACTOR EXPERIMENT
SCHEMATIC FLOW DIAGRAM

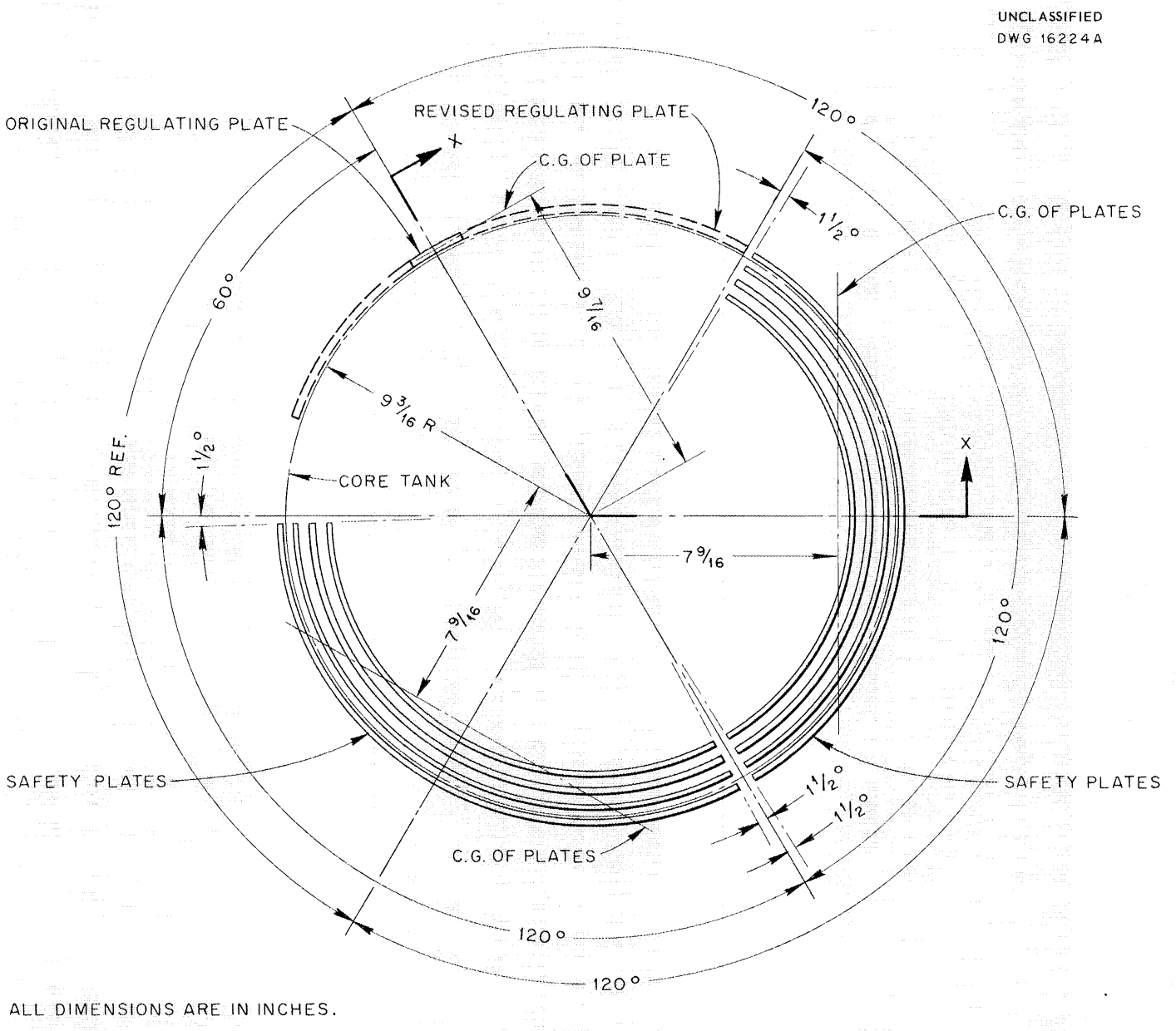

ALL DIMENSIONS ARE IN INCHES.

Fig. 3. Arrangement of Safety and Regulating Plates.

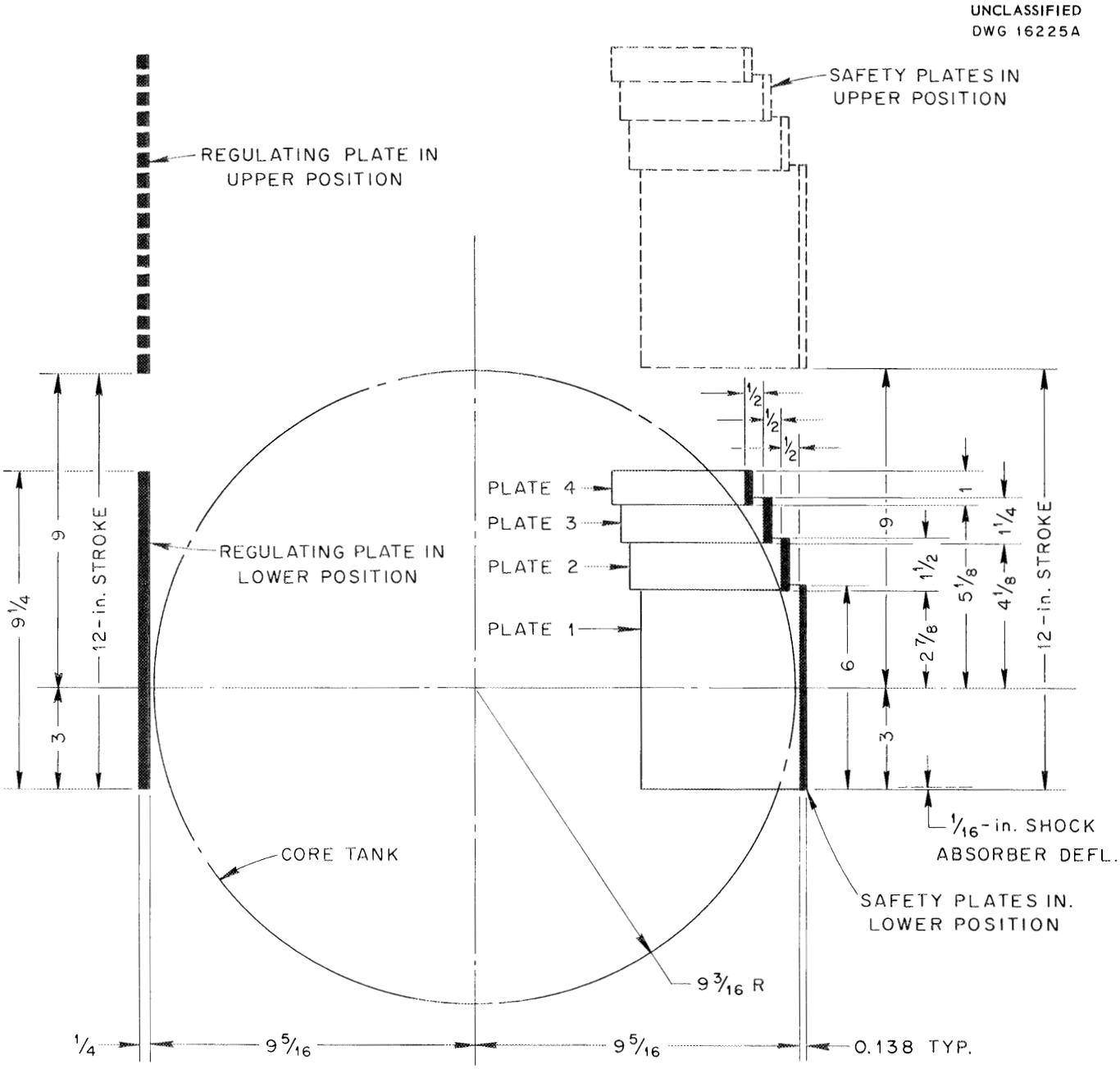

ALL DIMENSIONS ARE IN INCHES.

Fig. 4. Arrangement of Safety and Regulating Plates.

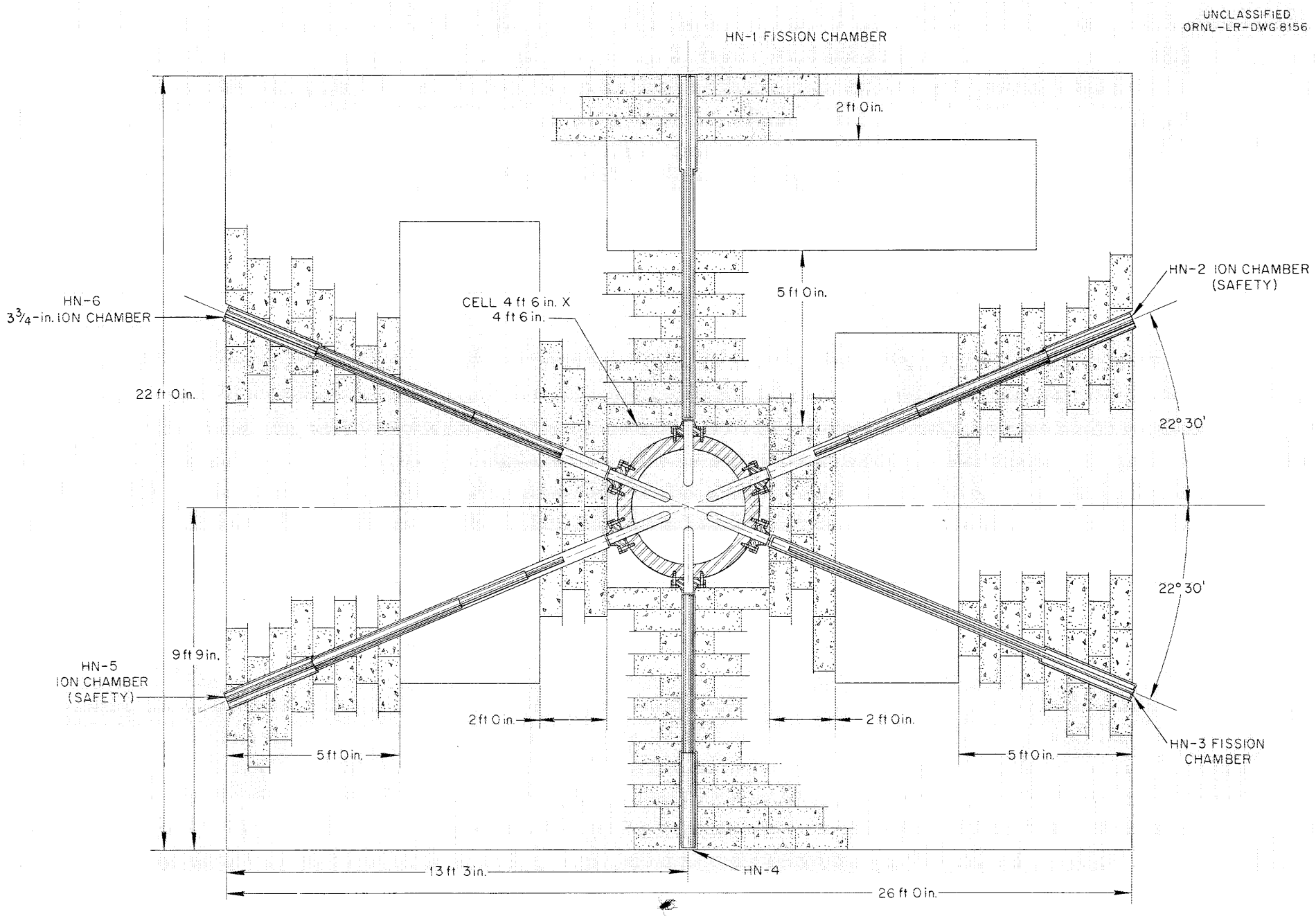

Fig. 5. Thimble for Nuclear Instruments.

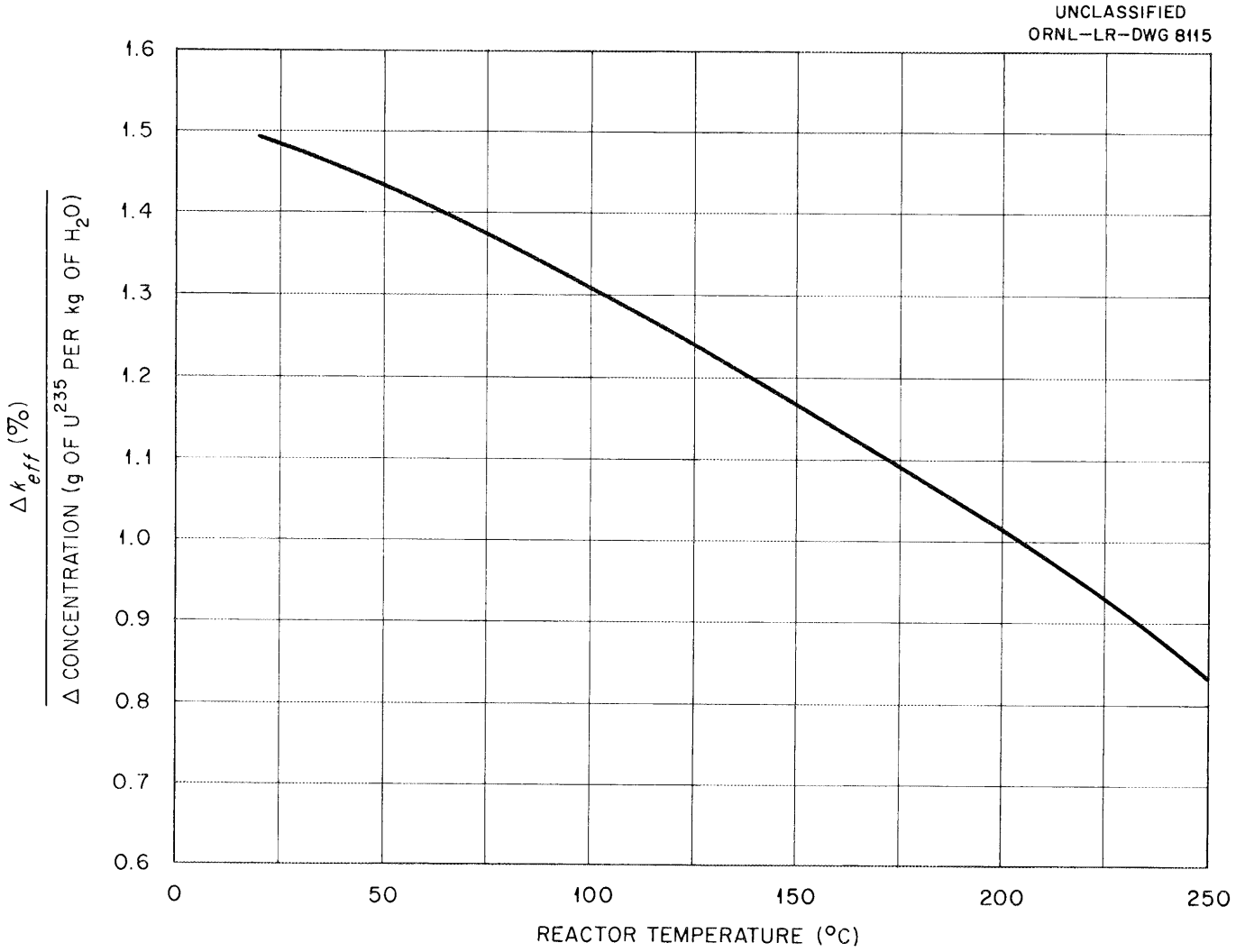

Fig. 6. Concentration Coefficient of Reactivity for HRE.

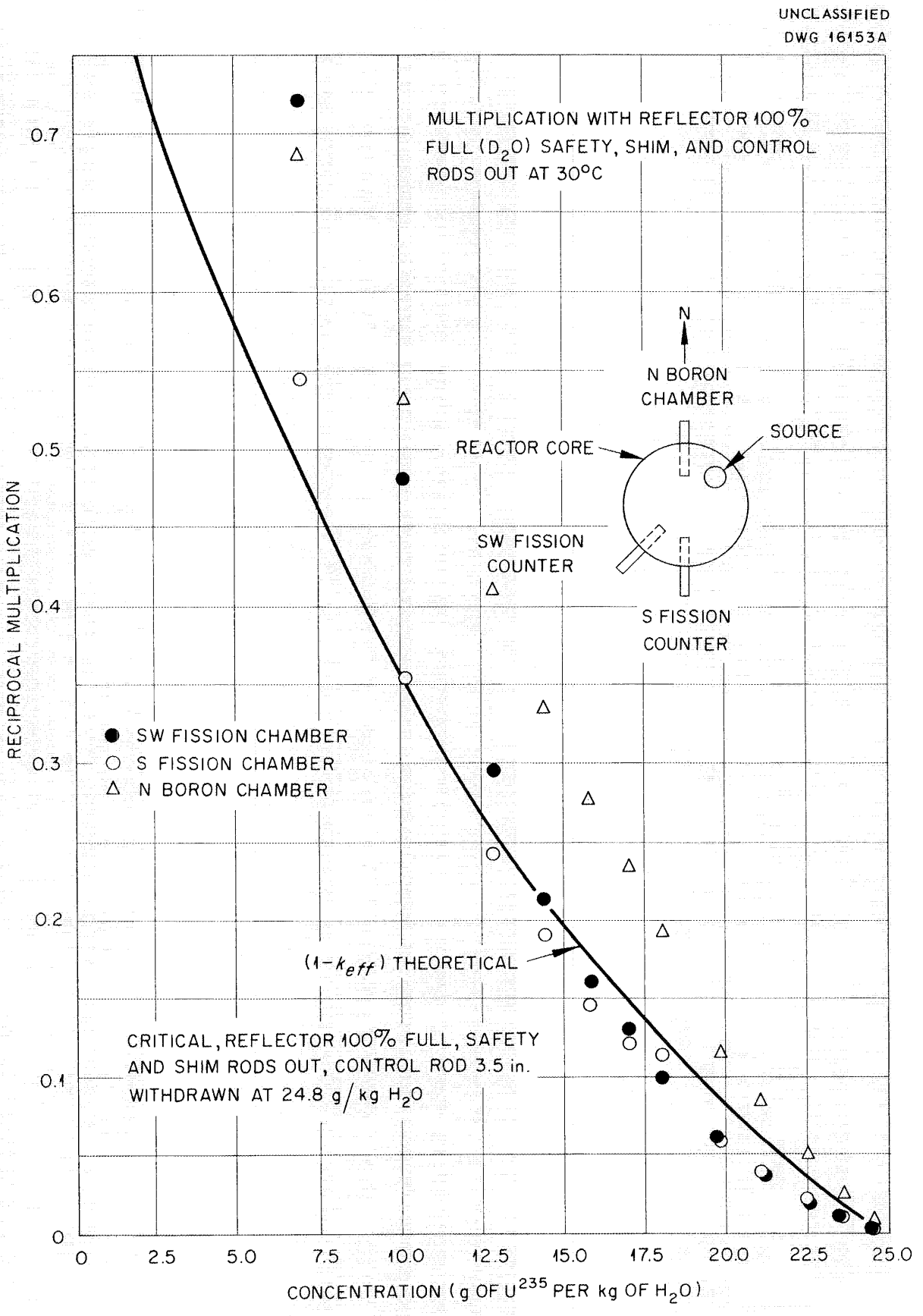

Fig. 7. Multiplication During Initial Critical Experiment.

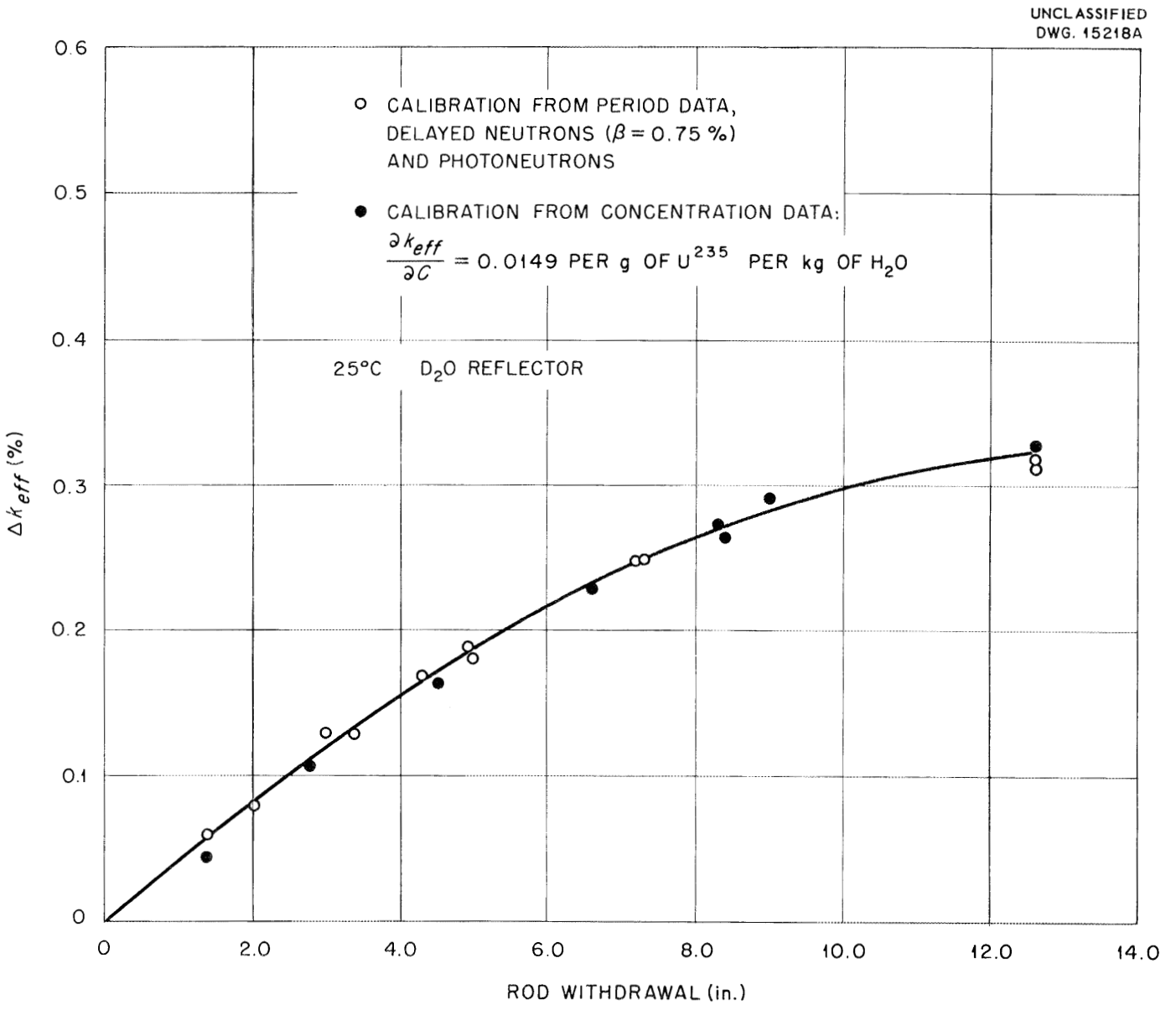

Fig. 8. HRE Control Rod Calibration at Room Temperature.

UNCLASSIFIED
DWG 15217B

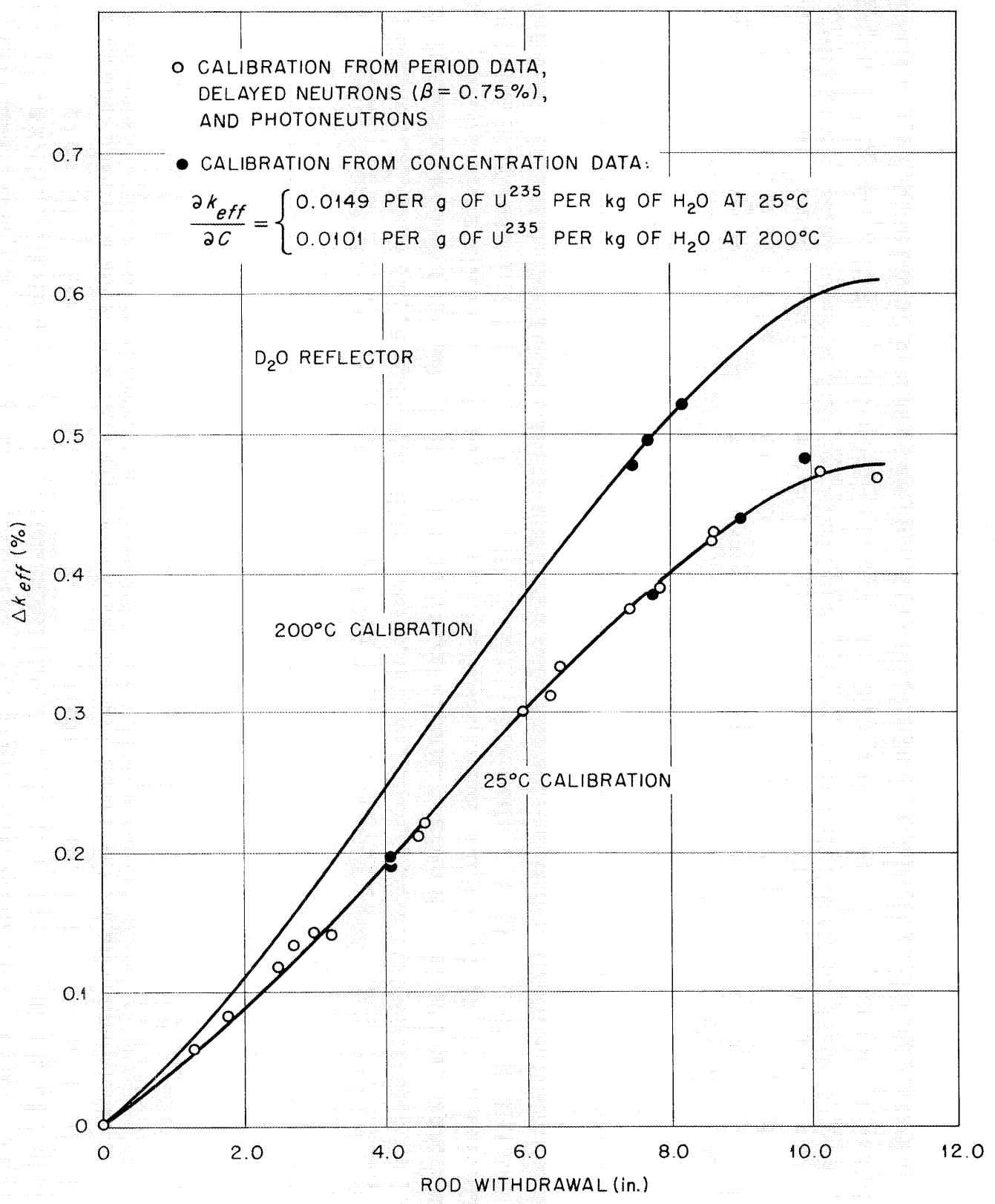

Fig. 9. HRE Shim Rod Calibration.

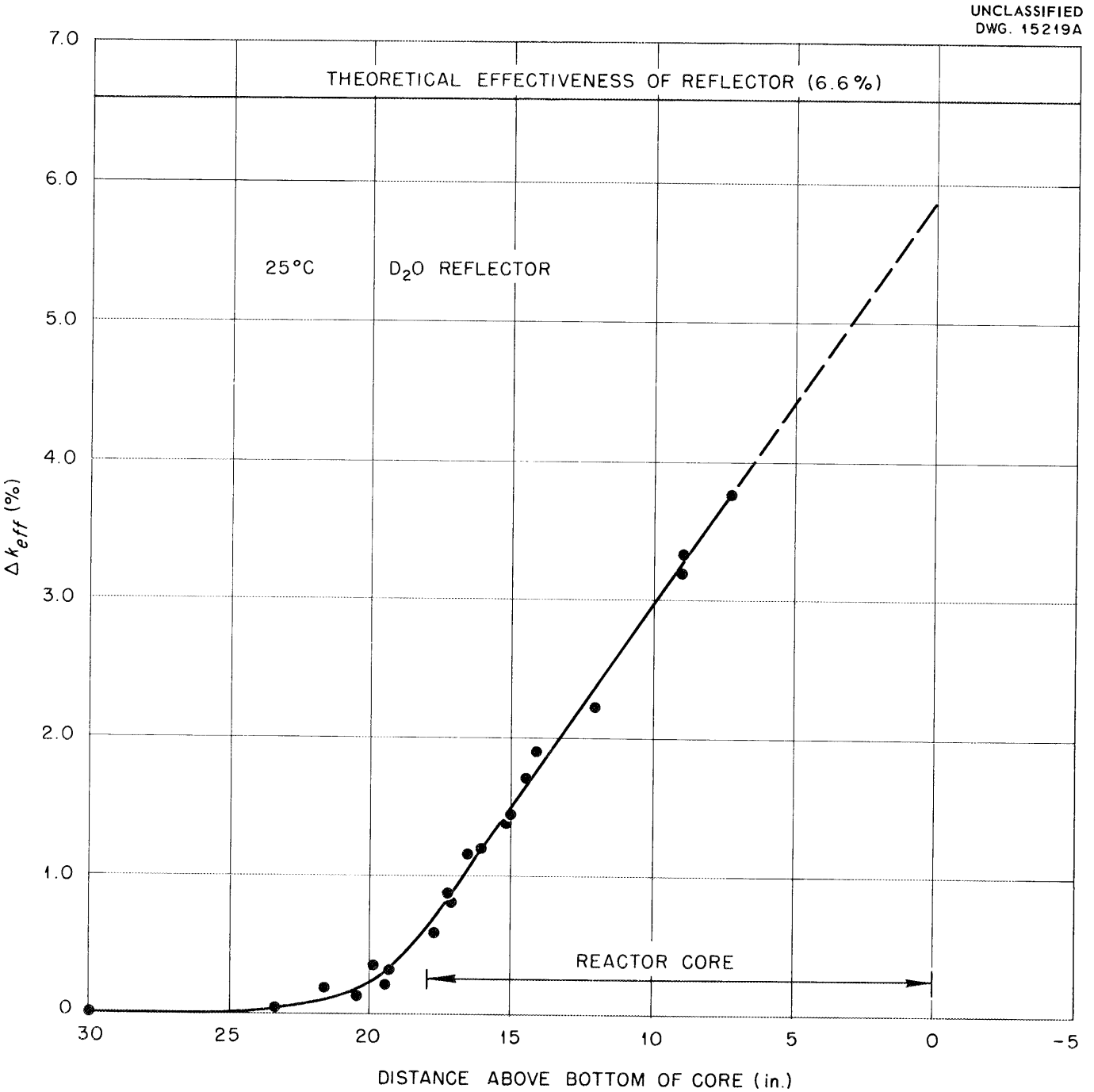

Fig. 10. HRE Reflector Calibration at Room Temperature.

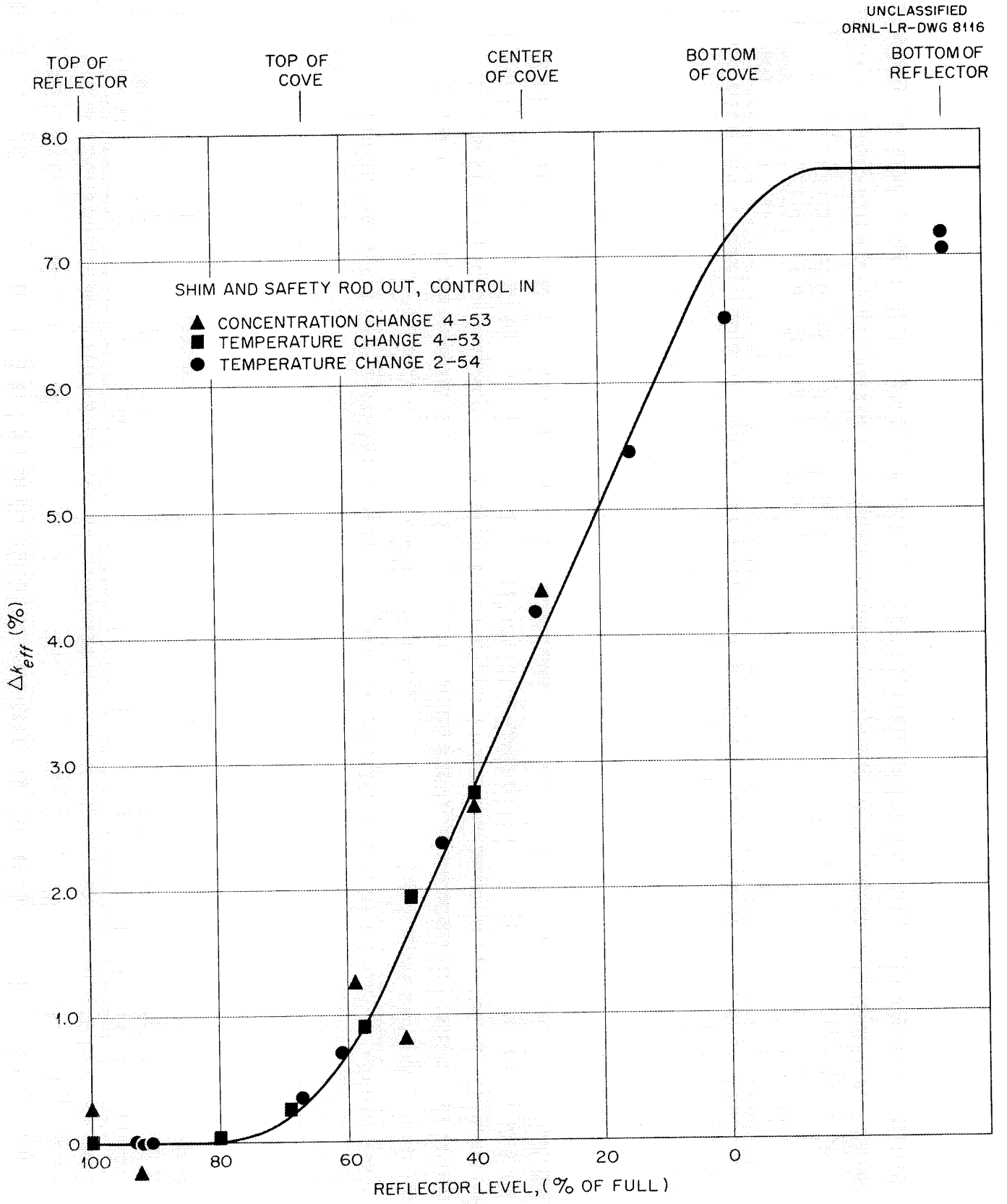

Fig. 11. Effectiveness of HRE Reflector at 225 °C

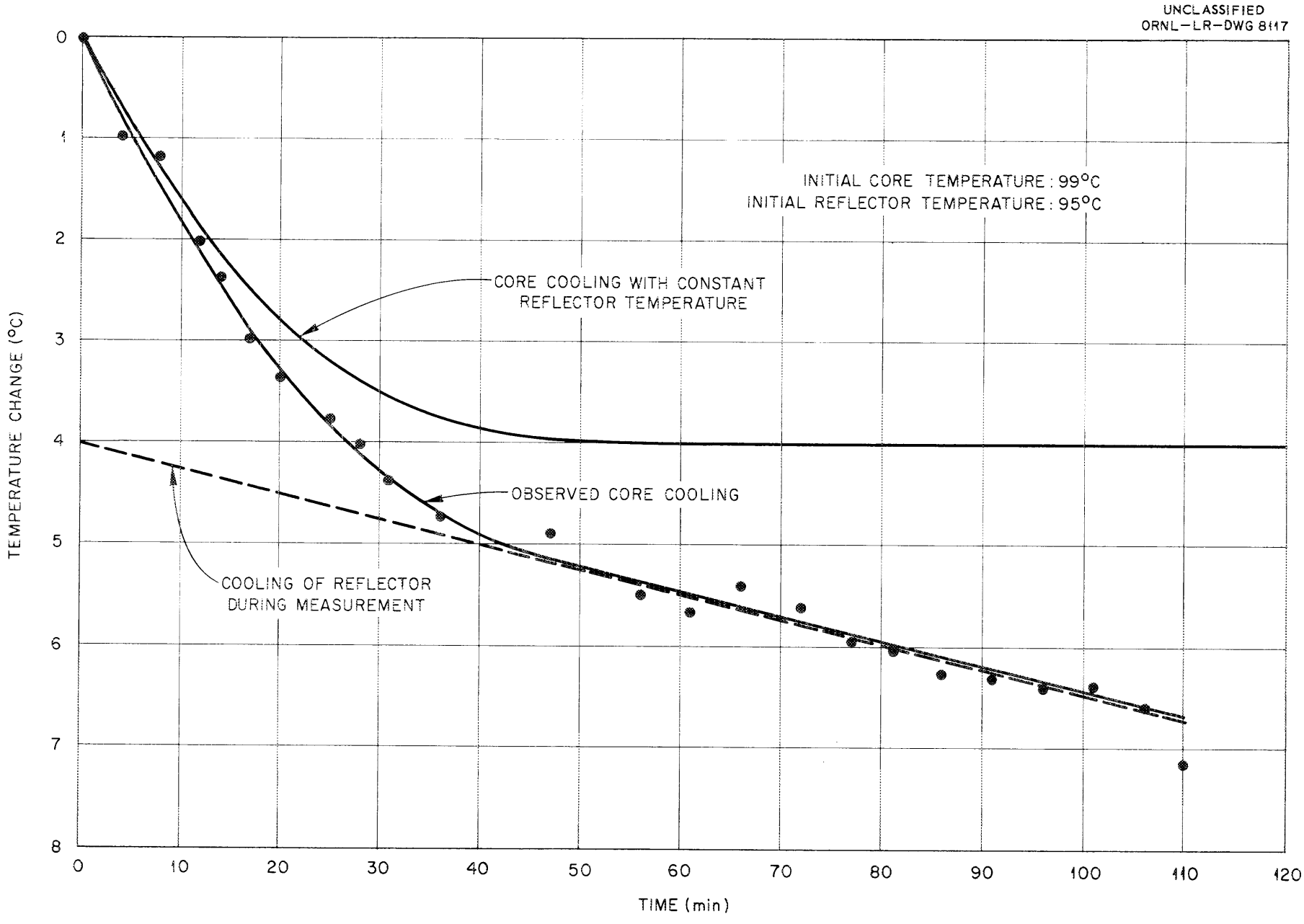

Fig. 12. Core Cooling After Stopping 100A Pump in HRE.

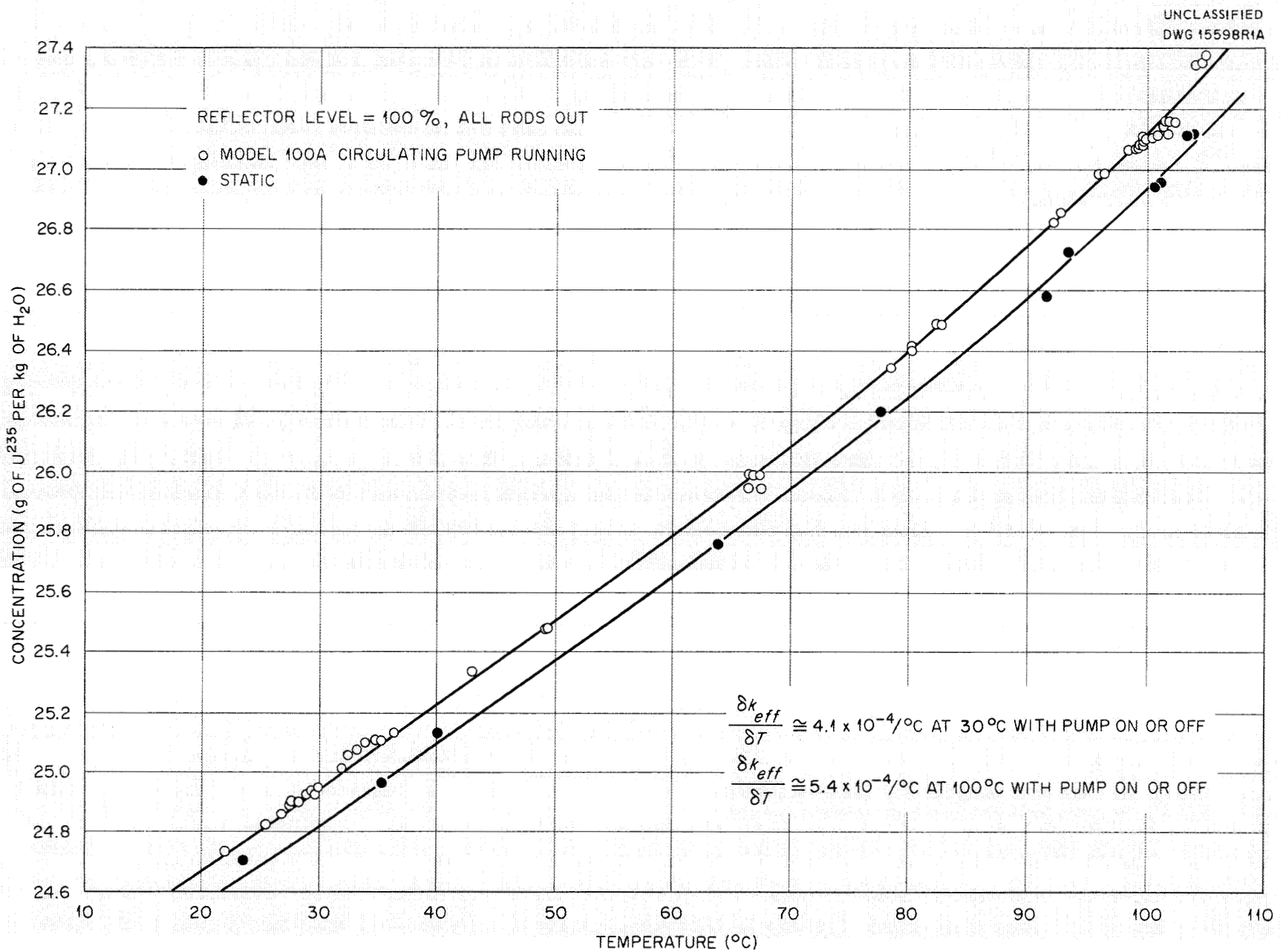

Fig. 13. Critical Concentration of HRE Below 105°C.

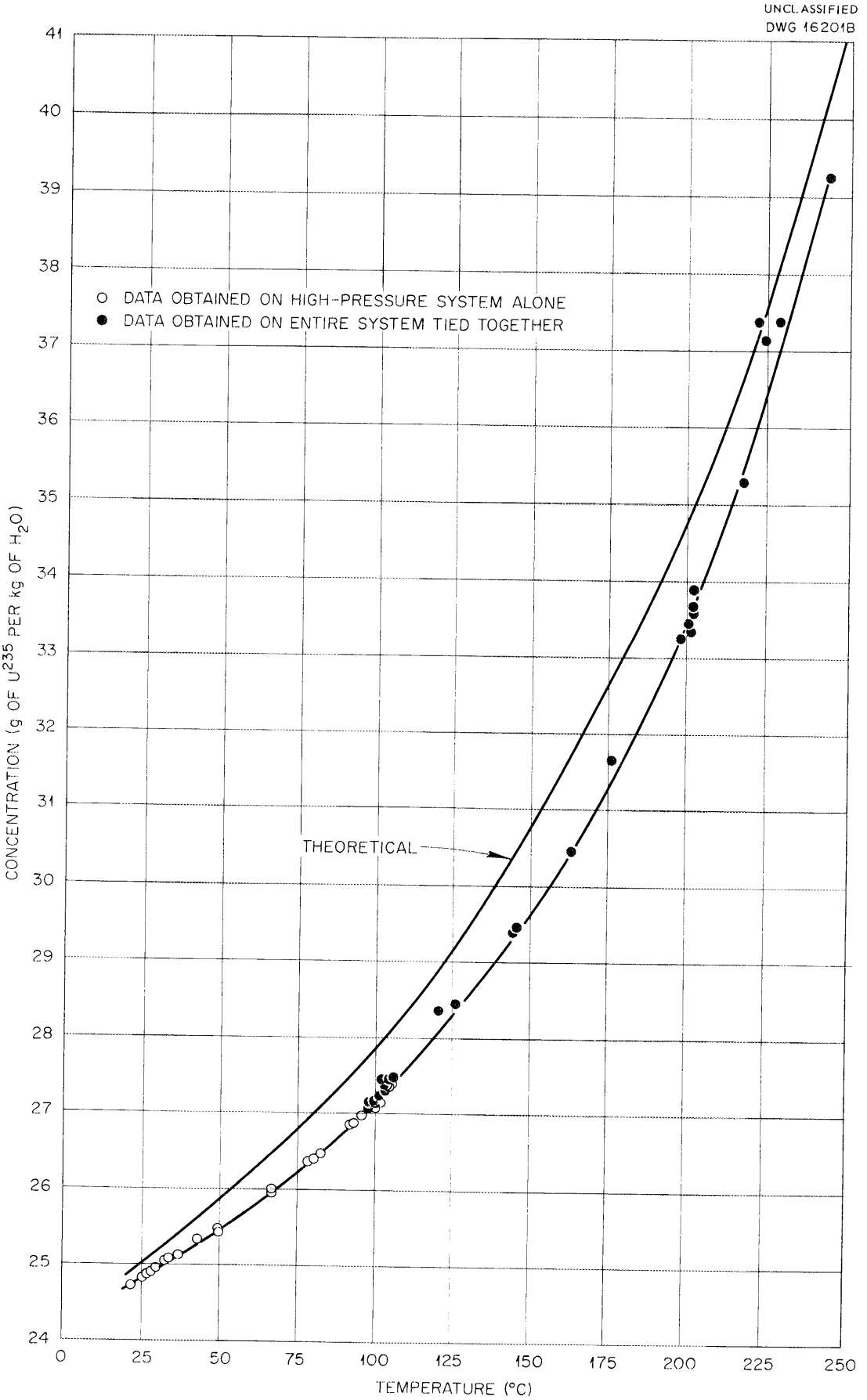

Fig. 14. Critical Concentration of HRE at all Temperatures.

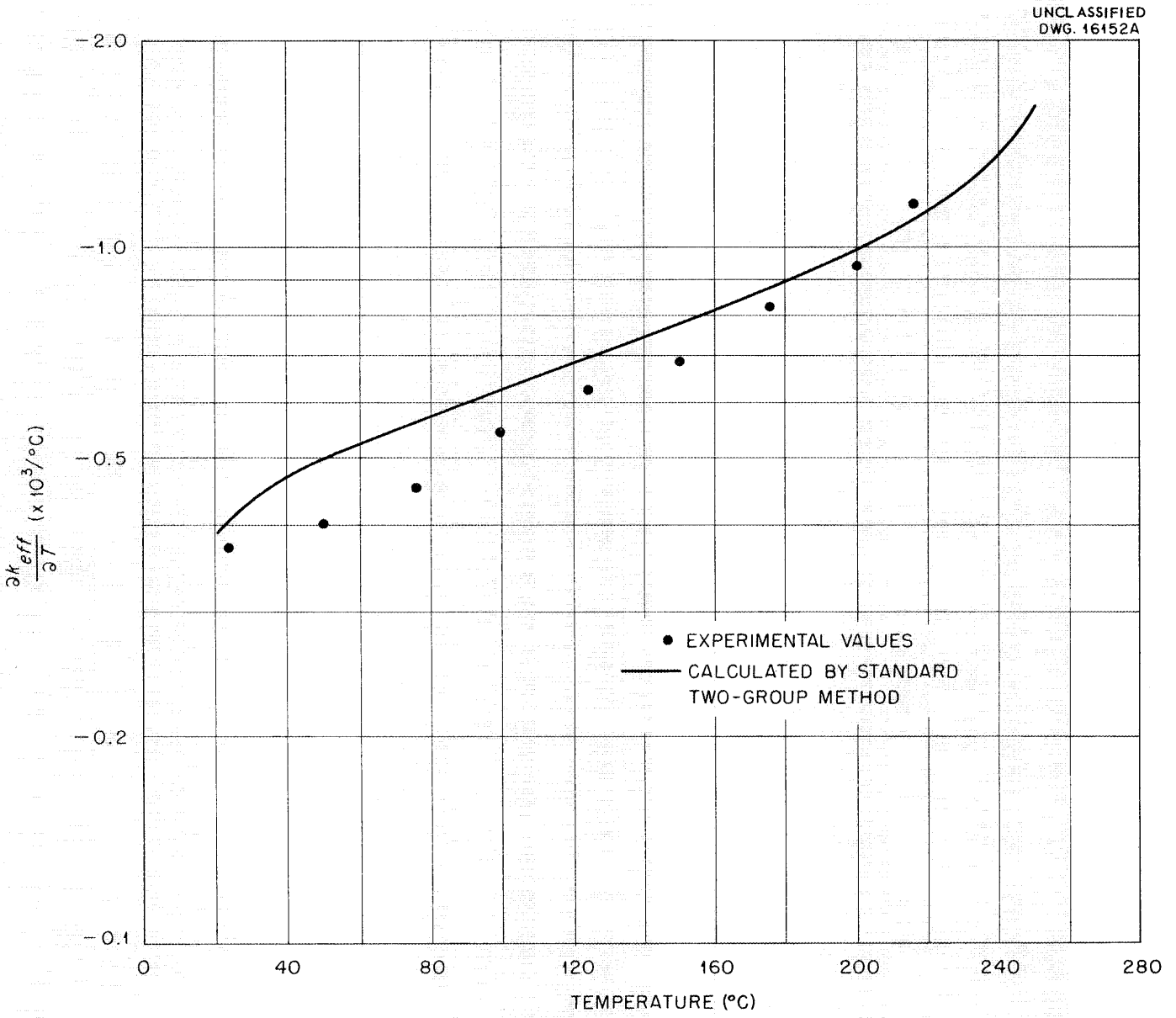

Fig. 15. Temperature Coefficient of Reactivity for the HRE.

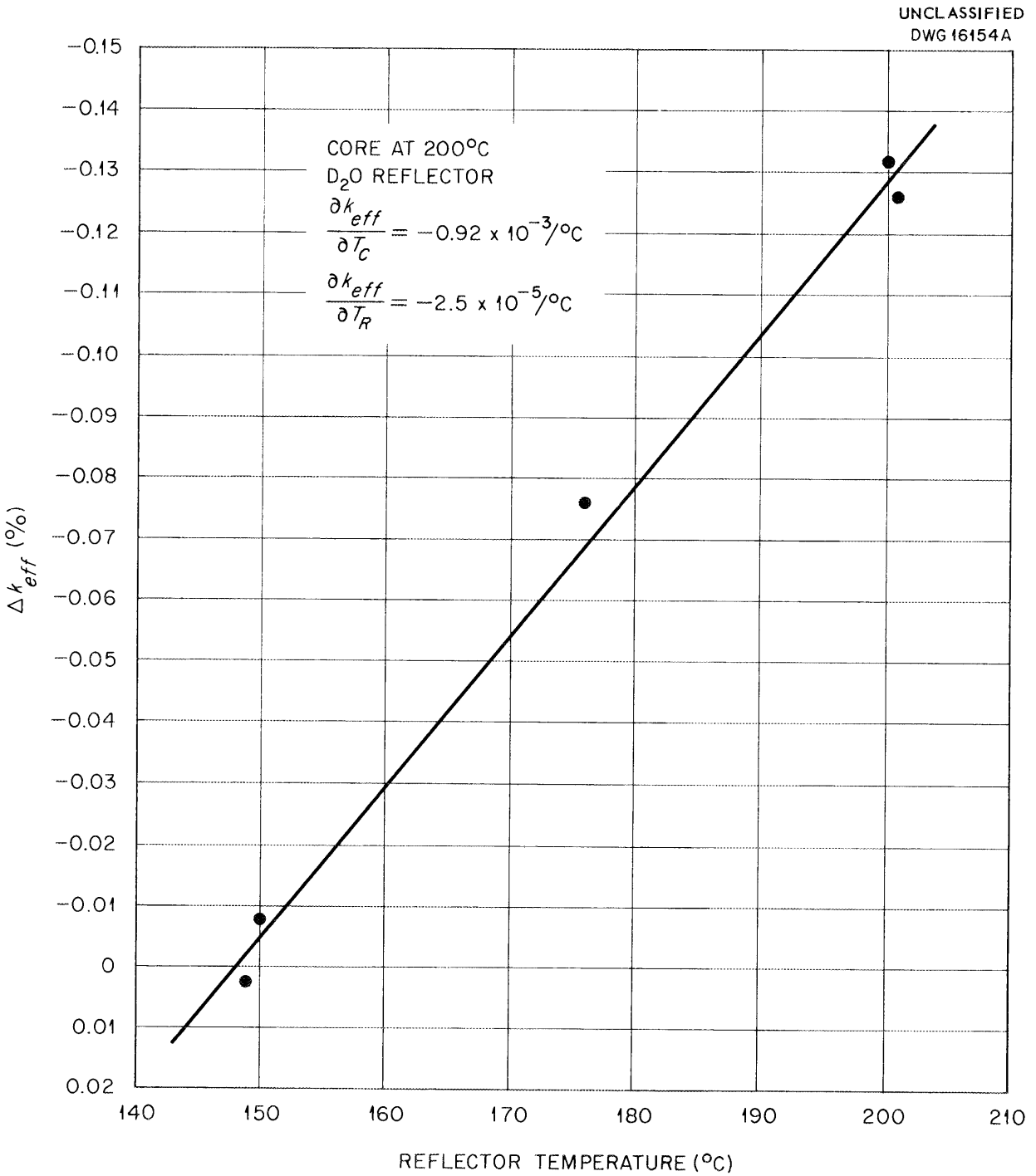

Fig. 16. Effect of Reflector Temperature on Reactivity.

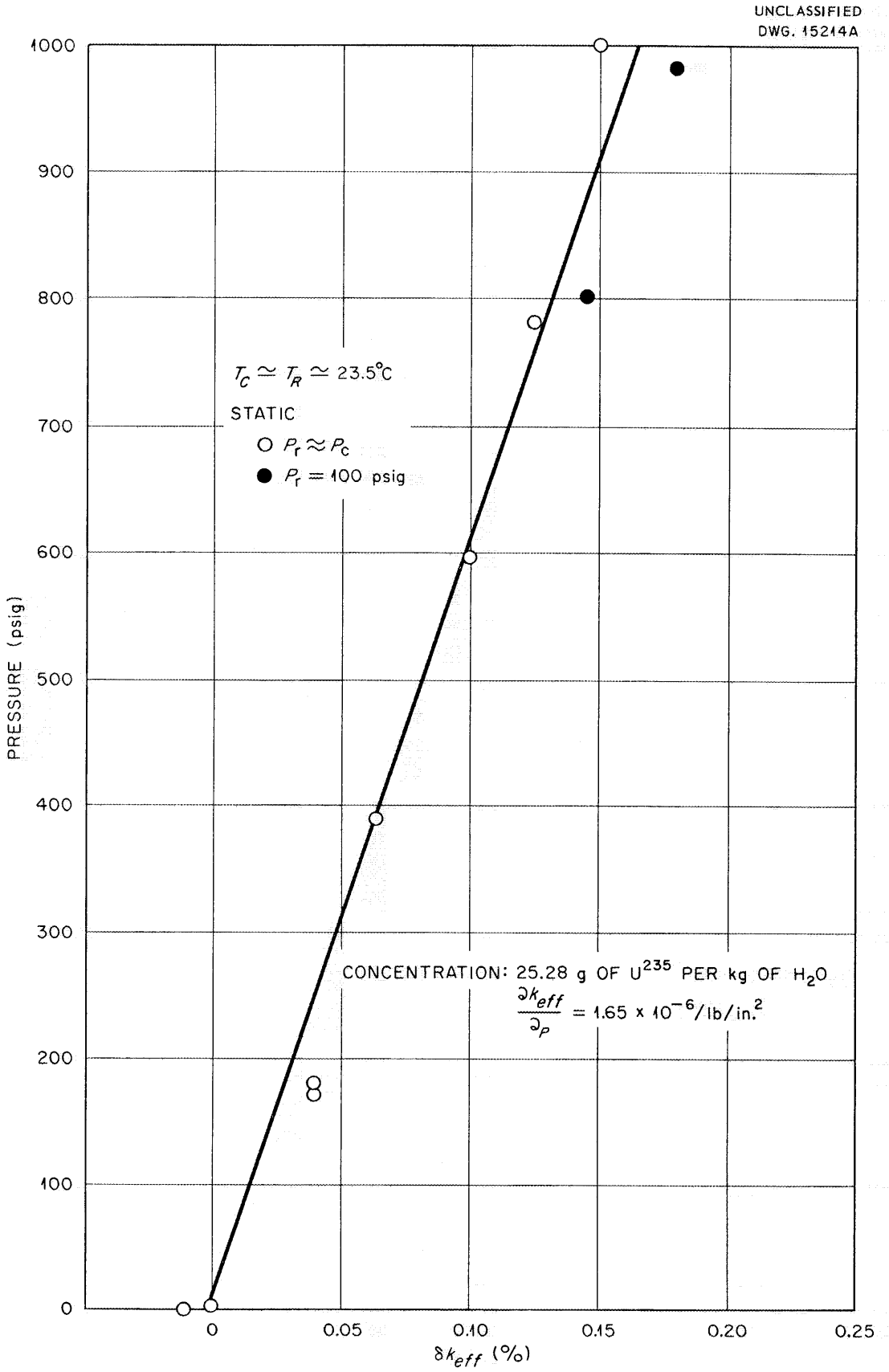

Fig. 17. Dependence of Reactivity on Pressure in the HRE.

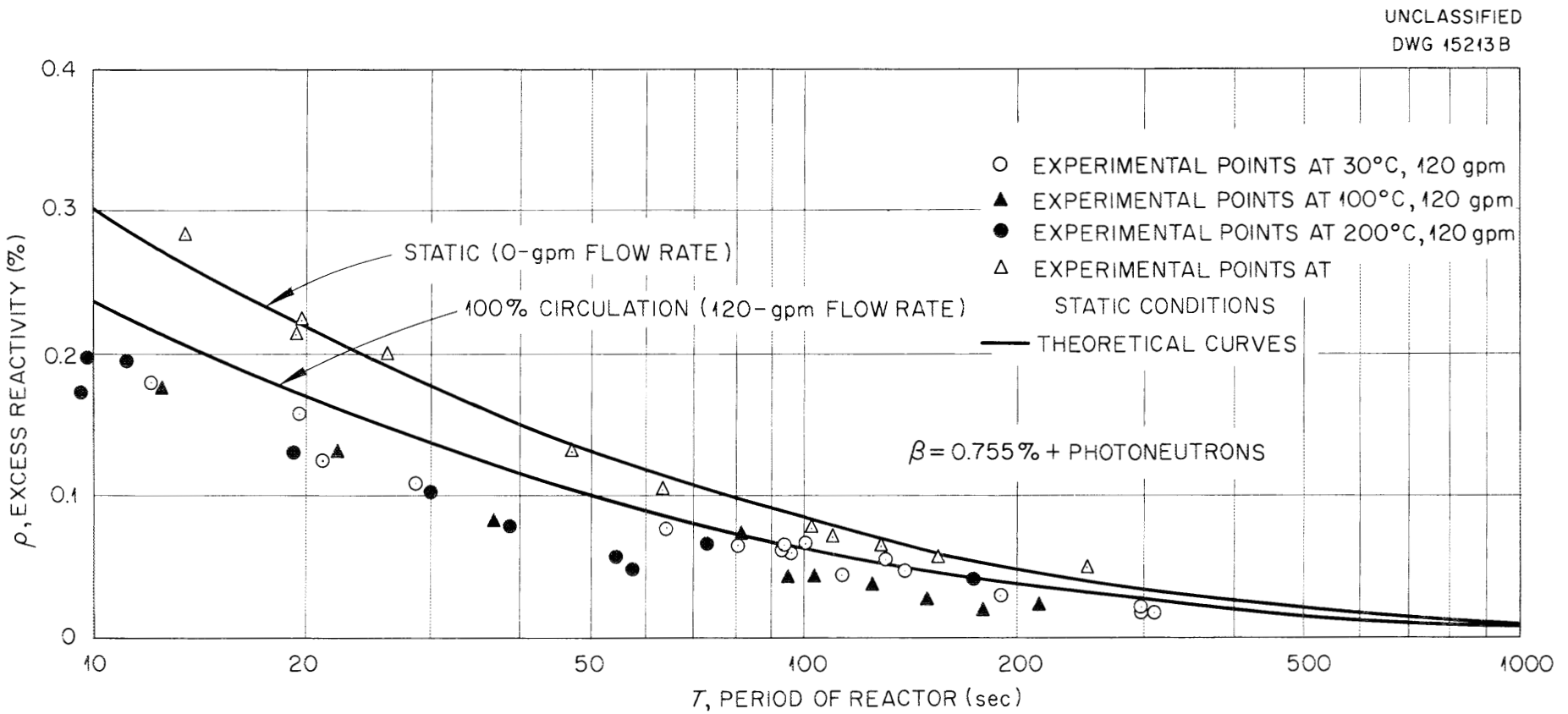

Fig. 18. Inhour Curves for the HRE.

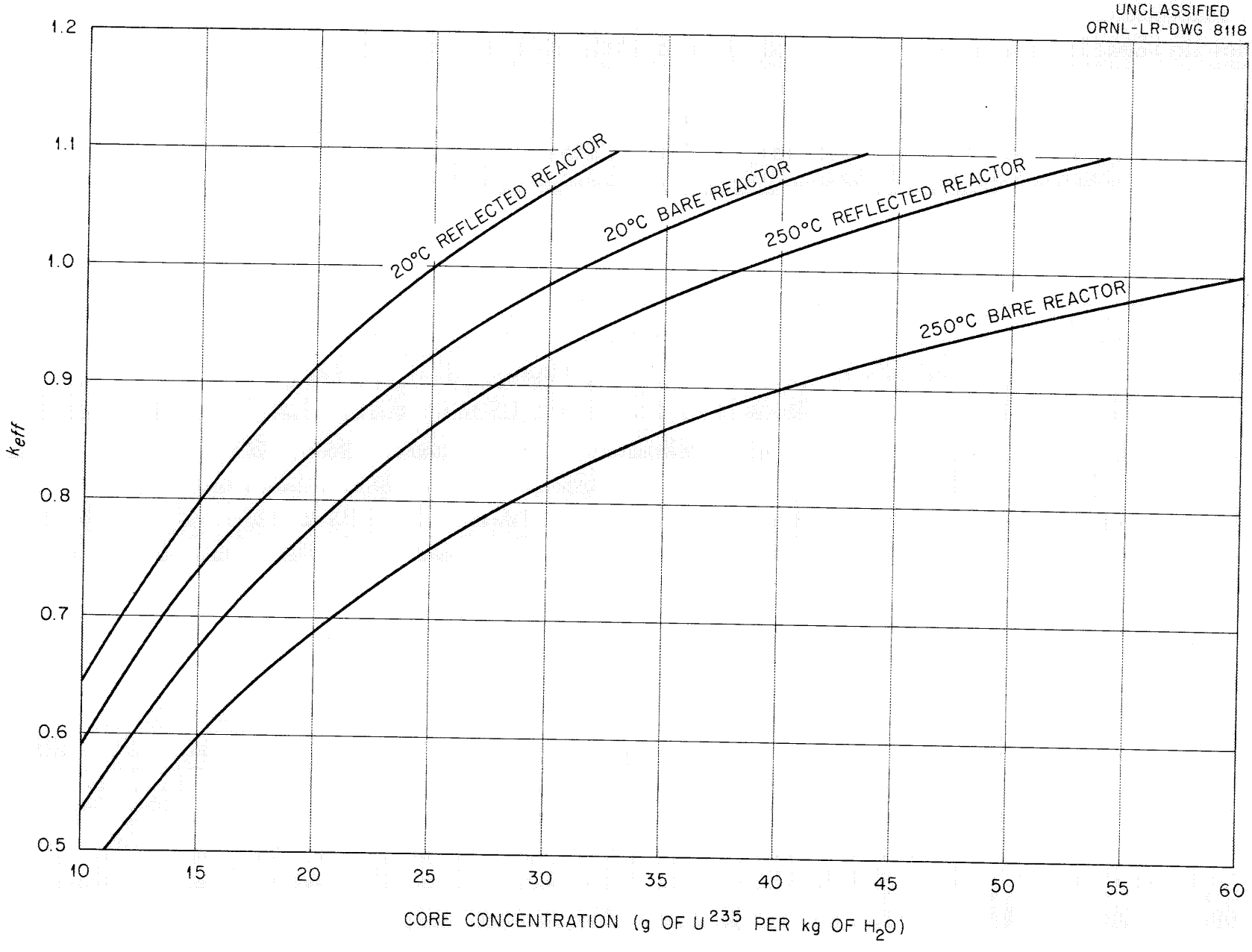

Fig. 19. Calculated Effect of Fuel Concentration of the HRE on Reactivity.

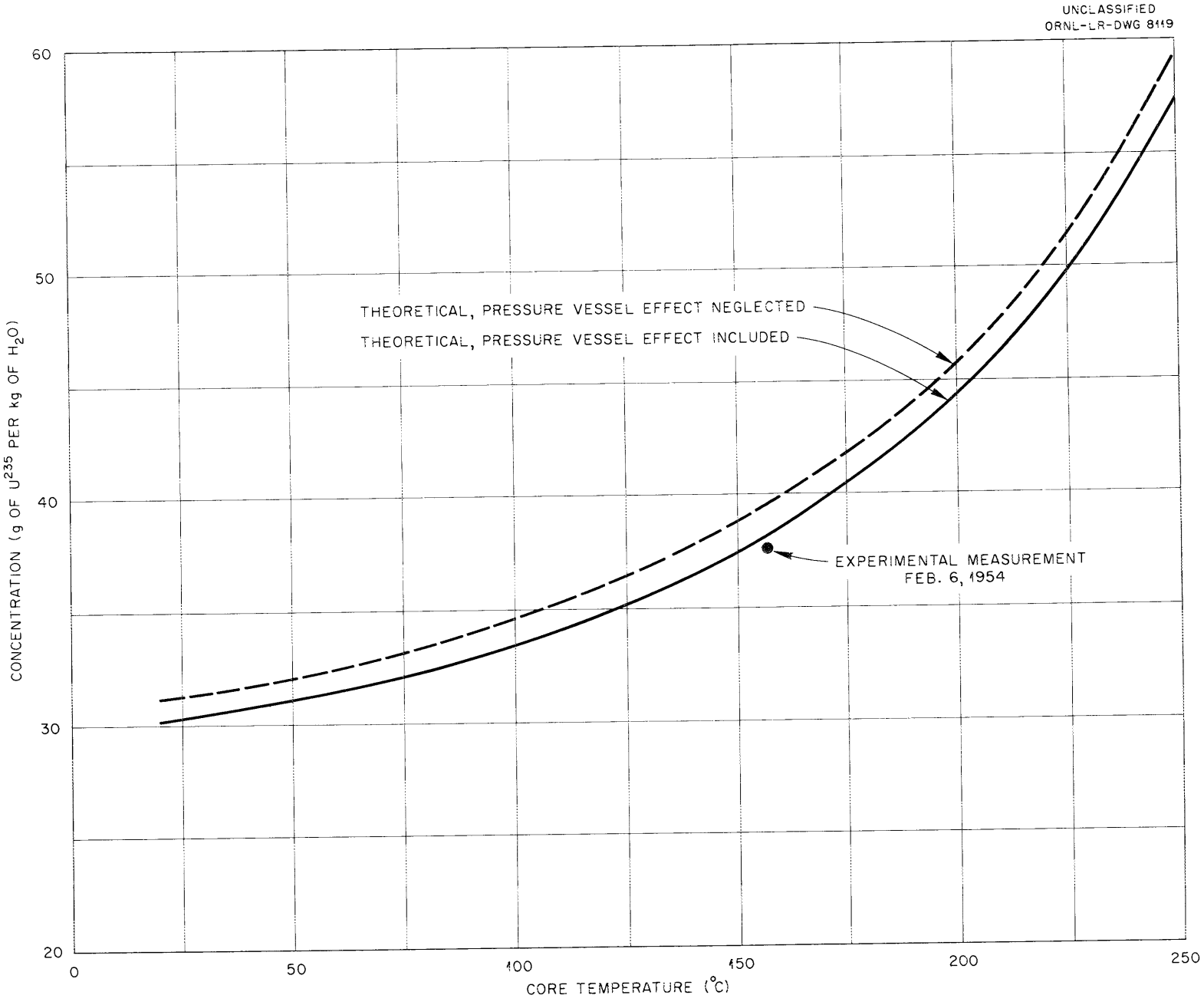

Fig. 20. Calculated Critical Concentration of the Unreflected HRE.

REFERENCES

1. Homogeneous Reactor Experiment Feasibility Report, ORNL-730 (Aug. 15, 1950).

2. HRE Design Manual, ORNL CF-52-6-160 (Nov. 18, 1952).

3. A Manual of HRE Control and Instrumentation, ORNL-1094 (Jan. 9, 1952).

4. HRE Operations Manual, ORNL CF-53-1-94.

5. T. E. Cole, E. E. St. John, S. H. Hanauer, The MTR Safety System and Its Components, ORNL-1139 (Apr. 25, 1952).

6. T. A. Welton, HRP Quar. Prog. Rep. Nov. 15, 1951, ORNL-1221

7. Appendix I; previously unreported.

8. R. P. Feynman and T. A. Welton, The Calculation of Critical Mass, LA-524 (Jan. 21, 1947).

9. E. Greuling and B. Spinrad, Critical Mass and Neutron Distribution Calculations, MonP-402 (Oct. 29, 1947).

10. Neutron Cross-Sections, AEC Advisory Group, BNL-170 (May 15, 1952).

11. F. J. Fisk, Transport Parameters for Thermal Neutrons in Water, ORNL-933 (March 15, 1951).

12. AEC Neutron Cross-Section Advisory Group, Neutron Cross-Sections, BNL-170 (May 15, 1952).

13. F. de Hoffman, Criticality of the Water Boiler and Effective Number of Delayed Neutrons, AECD-3051 (Dec. 8, 1944).

14. H. T. Williams, Photo-Neutron in the HRE, ORNL CF-51-12-122 (Dec. 19, 1951).

15. R. E. Aven, Delayed Neutrons and Their Reactivity Contribution to the Homogeneous Reactor, ORNL CF-51-12-1 (Dec. 4, 1951).

16. C. K. Beck, A. D. Callihan, et al., Critical Mass Studies, Part III, K-343 (Apr. 19, 1949).